

Injection moulded all-polypropylene composites composed of polypropylene fibre and polypropylene based thermoplastic elastomer

Kmetty A., Barany T., Karger-Kocsis J.

This accepted author manuscript is copyrighted and published by Elsevier. It is posted here by agreement between Elsevier and MTA. The definitive version of the text was subsequently published in [Composites Science and Technology, 73, 2012, DOI: [10.1016/j.compscitech.2012.09.017](https://doi.org/10.1016/j.compscitech.2012.09.017)]. Available under license CC-BY-NC-ND.

Injection moulded all-polypropylene composites composed of polypropylene fibre and polypropylene based thermoplastic elastomer

Ákos Kmetty^{1,2*}, Tamás Bárány², József Karger-Kocsis^{1,2}

¹MTA–BME Research Group for Composite Science and Technology, Muegyetem rkp. 3., H-1111 Budapest, Hungary

²Department of Polymer Engineering, Faculty of Mechanical Engineering, Budapest University of Technology and Economics, Muegyetem rkp. 3., H-1111 Budapest, Hungary

*corresponding author (Tel: (36-1)-463-1594, Fax: (36-1)-463-1527,
kmetty@pt.bme.hu)

Abstract

All-polypropylene composites comprising of polypropylene based thermoplastic elastomer (TPE) matrix and homo-polypropylene (hPP) fibre reinforcement were prepared and processed by injection moulding. For the injection moulding of plaque specimens pre-impregnated pellets, prepared by combined filament winding and film stacking were used. The processing-structure-property relationships of the all-PP composites were studied on specimens cut from the plaques produced at different melt temperatures (120, 140, 160°C). The properties determined covered the moulding-induced shrinkage, flexural stiffness via dynamic mechanical analysis, static tensile and high-speed perforation impact behaviours. It was demonstrated that by using TPE as matrix the processing window of this novel all-PP composite could be significantly increased. The static tests demonstrated that the yield stress and tensile modulus of the all-PP composites were prominently increased. Optical micrographs taken from polished sections of the composites confirmed good interfacial adhesion between the

matrix and the fibres. It was established that the shrinkage behaviour of the TPE based all-polypropylene composites is similar to that of conventional polypropylene.

Keywords A. MATERIAL: POLYMER-MATRIX COMPOSITES (PMCs),
B. PROPERTY: IMPACT BEHAVIOUR, B. PROPERTY: MECHANICAL
PROPERTIES, E. PROCESSING: INJECTION MOULDING,
ALL-POLYPROPYLENE COMPOSITES

1 Introduction

Fibre-reinforced rubber composites have widely been used. Most systems employed continuous and short fibres because of improved properties of the composites. Various studies were published on short fibre reinforced composites which include rayon, p-aramid (Kevlar) m-aramid (Nomex), polyester and glass fibres [1-2]. Recently thermoplastic elastomers (TPEs) have been applied as matrix materials to produce discontinuous natural and man-made fibre-reinforced composites. TPEs can be made by copolymerization (resulting in block or graft copolymers) or by blending techniques [3-4]. In blending usually a thermoplastic polymer is combined with a suitable elastomer material. The thermoplastic polymer forms the continuous phase whereas the elastomer is the dispersed one. Polyolefin-based TPEs with “dispersed elastomer” phase can also be produced by copolymerization. Using TPE as matrix and thermoplastic fibres as reinforcement composites with a wide processing window can be produced because the melting temperature of semicrystalline TPE materials is very low (~80-100°C) compared to semicrystalline thermoplastic fibres (~130-260°C) [5-6]. Their combination opens a new horizon for the industrial production of all-polymer composites. Nowadays, all-polymer and self-reinforced materials/composites [7] can be produced with narrow processing window by hot compaction (single-component self-

reinforced materials (SRM)) [8-11], consolidation of coextruded tapes [12-14] and film-stacking methods (multi-component SRM) [15-21]. In addition, all of the above processing methods yield sheet-like (pre)products which can be shaped thereafter by thermoforming. Three-dimensional parts with complex geometry cannot be produced and thus the most design-friendly and versatile processing, i.e. injection moulding, cannot be adapted. Therefore considerable efforts are in progress to produce injection-mouldable self-reinforced polypropylene composites.

In this article we describe the preparation of injection mouldable all-polypropylene composites by using polypropylene-based thermoplastic elastomer as matrix material and high-tenacity polypropylene (PP) fibre as reinforcement, and report on their processing-structure-property relationships.

2 Materials, their processing and testing

2.1 Materials

Highly oriented polypropylene homopolymer (hPP) multifilament (Stradom S. A., Czestochowa, Poland) was selected and used as reinforcement. This reinforcing multifilament had a melting temperature of 173°C (determined by DSC), single fibre diameter of 40.1±1.8 µm, tensile strength of 581±30 MPa and tensile modulus of 6432±490 MPa (measured in single fibre tensile tests).

As matrix material polypropylene-based thermoplastic elastomer (TPE) (Versify 4200, Dow Chemical Company) was selected and used. According to Fourier Transform Infrared Spectroscopy (FTIR) this TPE was a propylene-ethylene copolymer. Its Melt Flow Index (MFI) was determined with a CEAST Melt Flow Modular Line instrument according to the MSZ EN ISO 1133:2005 standard with a load of 2.16 kg at different temperatures (120, 130, 140, 150 and 160°C). MFI increased linearly (between 1.0-3.9

g/10 min) as a function of the temperature at least in the investigated temperature range. From the TPE pellets a 50 µm thick foil was prepared by extrusion film-blowing.

The advantage of the present material combination is the wide processing window, approximated by the difference between the melting temperatures of the reinforcement and matrix (ca. 90°C). This is much larger than that of all the other material combinations using matrix and reinforcing materials from the same polymer family (less than 30°C). Figure 1 shows the melting/cooling curves of the matrix and reinforcement which were determined on a DSC Q2000 (TA Instruments, New Castle, USA) machine with heating/cooling rates of 10°C/min in the temperature range of -100...200°C.

To produce self-reinforced PP composites the most straightforward method is to exploit the polymorphism of PP whereby ca. 15-20°C difference between the melting temperatures of the matrix and reinforcements can be achieved [22]. In case of all-PP composites usually PP homopolymer reinforcement is combined with a random PP (rPP) copolymer (containing 3...5 wt% ethylene) as matrix in order to ensure the processability (melting temperature difference: ca. 20°C for this material pair). Note that the terms self-reinforced PP and all-PP make a distinction between composites composed of the same polymer and of the same polymer family, respectively. It is intuitive that by using suitable polypropylene based thermoplastic elastomer the processing window of the all-PP version can be further widened. Since the components of all-PP composites belong to the same polymer family, the TPE itself should also be based on PP. To compare the selected Versify type TPE with the Tipplen R959A-type (TVK, Tiszaújváros, Hungary) PP copolymer (which was used in our previous study [23]) FTIR tests were performed on Bruker Tensor 27 spectrophotometer on the matrix

foil (50 μm thick) in a wave number range: 4000...400 cm^{-1} with resolution of 2 cm^{-1} . Figure 2 compares the FTIR spectra of the Tipplen R959A random polypropylene copolymer and Versify thermoplastic elastomer. Comparing the FTIR spectra of PP copolymer (R959A) and PP-based TPE (Versify) in Figure 2, one can observe differences only in the intensities of the peaks. This refers to higher ethylene content of the thermoplastic elastomer than of the rPP. It is important to note that no other peak can be found.

2.2 Pre-impregnated material preparation

The matrix film and the reinforcing PP multifilament were laminated to an aluminium core using filament winding combined with film-stacking. Note that the orientation of the filament was unidirectional in between the TPE foil layers. Afterward, the corresponding “package” has been consolidated by compression moulding (Figure 3). TPE/hPP sheets with a thickness of 1.6 mm and 70 wt% nominal reinforcement content were produced by compression-moulding. The consolidation process took place as follows: after heating up the mould to 140°C, the wound, film-stacked package was inserted and held for 240 s without pressure and for 480 s under pressure of 5.26 MPa, and then it was cooled to 45°C. The consolidated sheets were chopped into small pellets having a dimension of 5x5 mm which were used for injection moulding. The consolidated sheet had a yield stress of 250 \pm 18 MPa and tensile modulus of 2330 \pm 226 MPa (measured in tensile tests with 5 mm/min crosshead speed on 150x25mm (length x width) rectangular specimens). The cross section of the sheet is shown in Figure 4. The SEM picture in Figure 4 indicates that the impregnation of the hPP fibres was good. No voids could be observed between the single hPP fibres and the TPE matrix material.

2.3 Injection moulding

From the pre-impregnated pellets 2.1 mm thick 80x80 mm plaque specimens (Figure 5) were injection moulded at different melt temperatures (120, 140, 160°C) using an Arburg Allrounder 370S 700-290 injection moulding machine. In this process a fan gate and a heated flat nozzle with 4 mm diameter hole was applied. To decrease the friction heat in the gate region a 2 mm thick gate was applied. The injection moulding parameters were the following: injection volume: 44 cm³; injection rate: 50 cm³; injection pressure: 800±200 bar; switch over point: 10 cm³; holding pressure: 400 bar; holding time: 10 s; residual cooling time: 15 s; screw rotational speed: 15 m/min; back pressure: 20 bar; decompression volume: 5 cm³; decompression rate: 5 cm³/s; melt temperature: 120/140/160°C; mould temperature: 20°C.

2.4 Specimens and their testing

Shrinkage tests

The shrinkage was measured after injection moulding at different times (1, 4, 24, 48, and 168 h) and positions on the plaque specimens by digital calliper (Figure 5).

Dynamic mechanical analysis (DMA)

The DMA tests were performed on DMA Q800 (TA Instruments, New Castle, USA) machine with using 3 point bending clamp with the following parameters: Frequency: 1 Hz; temperature range: -100...70°C, amplitude: 160 µm; heating rate: 5°C/min. For the tests 60x10x2 mm specimens were applied which were cut from the plaque specimens in the flow direction (side) by waterjet cutter.

Static tensile tests

Static tensile tests were performed on the pre-impregnated sheets (20x150 mm) and on injection moulded plaque specimens, as well. From the 80x80 mm plaque specimen dumbbell shape specimens (EN ISO 8256 type 3) were cut off in both the flow direction

and perpendicular to it by waterjet cutting (see Figure 6 for specimen locations). Tensile tests were carried out on a universal ZWICK Z020 tensile machine according to the standard EN ISO 527. The cross-head speed was 5 mm/min and each test was performed at room temperature (24°C). At least five specimens were tested for each material.

Dynamic falling weight impact tests (IFWI)

Instrumented falling weight impact (IFWI) tests were performed on the injection moulded specimens on a Fractovis 3789 (Ceast, Pianezza, Italy) machine with the following settings: maximal energy: 131.84 J; diameter of the dart: 20 mm; diameter of the support rig: 40 mm; weight of the dart: 13.62 kg and drop height: 1 m. IFWI tests were done at room temperature (RT) and -30°C, respectively. At least ten specimens were tested from each material at a given testing temperature.

Light microscopy (LM)

Light microscopy (LM; Olympus BX51M) pictures were taken from polished cross section of the injection moulded specimens in both flow direction and perpendicular to it (Figure 6). Cross sections were cut from the injection moulded specimens and embedded in epoxy resin. After this the samples were polished in a Struers polisher in four steps using 320, 1000, 2400 and 4000 SiC papers and water as lubricant.

Scanning electron microscope (SEM)

Scanning electron microscopic pictures were taken from fracture surfaces on a JSM-6380LA (Jeol, Tokyo, Japan) microscope. The samples were sputter coated with gold alloy.

3 Results and discussion

3.1 Shrinkage tests

The shrinkage of the injection moulded specimens is demonstrated in Figure 7. The results show that the shrinkage data of the all-PP composites moulded at 120°C and 140°C are the same. The average shrinkage of the all-PP composite at 120°C and 140°C was ca. 0.8% which coincides well with the shrinkage value of conventional PP [24]. The highest shrinkage was detected in length direction in contrast to the glass fibre reinforced and glass bead filled products where the shrinkage (and warpage) in flow direction is decreased [25-27]. In case of 160°C the shrinkage of the specimens increased in length direction (side and middle section, too). This can be attributed to the relaxation of the thermoplastic fibres.

3.2 Dynamic mechanical analysis (DMA)

The storage modulus and $\tan\delta$ as a function of temperature are shown in Figure 8. The DMA traces prove that the TPE can be efficiently reinforced by hPP fibres. Increasing processing temperature was accompanied with a decrease in the storage modulus that was attributed to the heat relaxation of the hPP fibres. The glass transition temperature of the matrix ($T_g=-38^\circ\text{C}$ based on the $\tan\delta$ peak temperature) was broadened by the reinforcement and hardly any peak value could be exactly determined.

3.3 Static tensile tests

The Figure 9 shows the yield stress and tensile modulus of the all-PP composites. Using both compression and injection moulding the yield stress and the tensile modulus of the composites were increased significantly compared to the matrix material. Note that the static mechanical parameters of the injection moulded all-PP specimens agree with those of conventional hPP grades ($\sigma_Y=25-30$ MPa, $E=950-1000$ MPa [28]). Results of the tensile tests are shown in Table 1. It can be seen that the yield stress of the all-PP composites depended on the processing temperature and on the analyzed area of the

plaque. With increasing processing temperature the yield stress values of the composites slightly increased. Specimens injection moulded at 160°C showed a yield stress of about 30 MPa which is very close to that of conventional PP homopolymers [29]. The yield stress in the side region was higher than in middle region when measured in flow direction. The yield stress of the matrix did not show orientation dependence. The tensile modulus of the composite in flow direction was significantly increased compared to the TPE matrix. Furthermore, a difference between the moduli measured in the side and the middle regions of the moulded plaques, can also be stated for the composites.

Results in Table 1 suggest that the mould filling process affected the mechanical properties via the related fibre alignment. The yield stress perpendicular to the flow direction depended on the analyzed area. With increasing distance from the gate the yield stress increased and reached 35 MPa. The difference in the yield stress values in the front and the back regions were 12-15 MPa. For the tensile moduli of the all-PP composites, measured perpendicular to the flow direction, a significant difference was observed, too. This is again an effect of the fibre orientation which is different in different sections of the plaque. In back region of the all-PP composite tensile moduli of 900-1000 MPa were achieved. By contrast, the tensile modulus of TPE did not change either with the processing temperature or with the position of specimen cut-off.

3.4 Instrumented falling weight impact tests (IFWI)

The perforation energy at different testing temperatures for the matrix and all-PP composites are listed in Table 1. Note that the perforation energy decreased at both room temperature and at -30°C for the composites compared to the neat matrix. Nonetheless, all values exceed that of the conventional random PP copolymer (0.5-1 J/mm) [30]. The processing temperature had a small effect on the perforation energy of

the matrix and related composite at both testing temperatures. Most striking feature is that the matrix material at -30°C experienced markedly higher perforation energy than at room temperature. This is due to the fact that the testing temperature of -30°C is very close to the T_g of the TPE which is associated with some “embrittlement”. Recall that according to the DMA results the storage modulus (see Figure 8) increases already in the vicinity of T_g (-38°C). This caused the higher force values than at room temperature in the related IFWI fractograms (cf. Figure 10). For ductile polymers the toughness reaches a maximum at the T_g (which is frequency dependent itself). Note that the frequency range of the IFWI test is in kHz range (cf. Figure 10) which means already a shift in the T_g toward higher temperatures compared to the DMA (frequency: 1 Hz). However, the typical failure occurred by plastic deformation of the TPE at both testing temperatures [31].

3.5 Light microscopy (LM)

LM frames taken from the polished cross sections of the all-PP composites produced at different melt temperatures are shown in Figure 11. The LM pictures in Figure 11 evidence that with increasing process temperature the all-PP composites became better consolidated. On the cross section no visible skin-core effect can be found in contrast to injection moulded parts with rigid discontinuous fibres (such as glass) [32]. This effect may be attributed to the high fibre content (70 wt%) and the flexible reinforcing fibres. The single fibres from the multifilament structure are disjoined gradually and form quasi homogenous structure. Pictures from the central zone in flow direction show that the single fibres are not laying perpendicular to the analyzing plane. LM pictures taken from the front region in direction perpendicular to the flow (Figure 12) showed the presence of skin layers. Their formation was likely caused by the thickness difference

between the specimen (2.1 mm) and the fan gate (2 mm). It is the right place to underline that using a 2 mm thick fan type gate markedly contributed to the reduction of heat generation in the gate section and thus to the maintaining of the hPP fibres. The residual length of the hPP fibres could not be determined on the polished section due to their complex orientation in space.

3.6 Scanning electron microscopy (SEM)

Figure 13 shows the fracture surfaces (after tensile tests) of the all-PP composites injection moulded at different melt temperatures. Similar to the LM pictures a quasi homogenous distribution of individual fibres can be found in the cross section, however, without any skin-core formation. The reinforcing hPP fibres are well impregnated by the matrix and between them good adhesion exists (Figure 14). SEM pictures in Figure 14 support that the good mechanical performance of the all-PP composites is guaranteed by the good fibre/matrix adhesion.

4 Conclusions

The goal of this study was to show the feasibility of the production of injection-mouldable all-polypropylene composites composed of a polypropylene-based thermoplastic elastomer (TPE) as matrix and highly oriented polypropylene homopolymer (hPP) multifilament as reinforcing material. A further aim was to investigate the morphological, static and dynamical mechanical properties of the composite. From the results it can be stated that PP-based thermoplastic elastomer is a suitable matrix material for all-polypropylene composites, since it ensures a wide processing window ($\sim 90^{\circ}\text{C}$). This processing window is by $50\text{-}70^{\circ}\text{C}$ higher than that of the conventionally applied technologies (hot compaction, co-extrusion and film-stacking method). The shrinkage of the TPE based all-polypropylene composites was

comparable with that of conventional polypropylene. The thermoplastic hPP worked as efficient reinforcement and significantly increased the yield stress and tensile modulus of the corresponding composites. The perforation energy of the all-polypropylene composite exceeds the values of the convention polypropylene at room temperature and at -30°, as well. Use of a 2 mm thick fan gate decreased the evolved heat in the gate region and thus contributed to the reinforcing efficiency of hPP fibres. Light microscopy pictures demonstrated good adhesion between the TPE matrix and the hPP fibres.

5 Acknowledgements

The authors want to thank the Hungarian Scientific Research Fund (OTKA K75117). T. Bárány is thankful for the János Bolyai Research Scholarship of the Hungarian Academy of Sciences. The work reported in this paper has been developed in the framework of the project "Talent care and cultivation in the scientific workshops of BME" project. This project is supported by the grant TÁMOP - 4.2.2.B-10/1--2010-0009. This work is connected to the scientific program of the "Development of quality-oriented and harmonized R+D+I strategy and functional model at BME" project. This project is supported by the New Széchenyi Plan (Project ID:TÁMOP-4.2.1/B-09/1/KMR-2010-0002). The authors are grateful to the Arburg Hungary Ltd for the delivery of the Arburg Allrounder 370S 700-290 machine used.

6 References

- [1] Saikrasun S, Amornsakchai T, Sirisinha C, Meesiri W, Bualek-Limcharoen S. Kevlar reinforcement of polyolefin-based thermoplastic elastomer. *Polymer*. 1999;40(23):6437-6442.
[http://dx.doi.org/10.1016/s0032-3861\(98\)00853-2](http://dx.doi.org/10.1016/s0032-3861(98)00853-2)
- [2] Westerlind B, Hirose S, Yano S, Hatekayama H, Rigdahl M. Properties of isoprene rubber reinforced with treated bleached kraft cellulosic fibers or rayon fibers. *Int J Polym Mater*. 1987;11(4):333-353.
<http://dx.doi.org/10.1080/00914038708078670>

- [3] Holden G. Understanding Thermoplastic Elastomers. Munich: Hanser; 2000.
- [4] Kresge EN. Polyolefin-Based Thermoplastic Elastomers. In: Holden G, Kricheldorf HR, Quirk RP, editors. Thermoplastic Elastomers. 3 ed, Munich: Hanser; 2004. p. 93-116.
- [5] Khalil AM, El-Nemr KF, Khalaf AI. Effect of short polyethylene terephthalate fibers on properties of ethylene-propylene diene rubber composites. *J Polym Res*. 2012;19(6):1-9.
<http://dx.doi.org/10.1007/s10965-012-9883-8>
- [6] Karger Kocsis J. Recycling options for post-consumer PET and PET-containing wastes by melt blending. In: Fakirov S, editor. Handbook of Thermoplastic Polyesters, vol. 2 Weinheim: Wiley-VCH; 2002. p. 1291-1318.
- [7] Kmetty Á, Bárány T, Karger-Kocsis J. Self-reinforced polymeric materials: A review. *Prog Polym Sci*. 2010;35(10):1288-1310.
<http://dx.doi.org/10.1016/j.progpolymsci.2010.07.002>
- [8] Ward IM. Developments in oriented polymers, 1970-2004. *Plast Rubber Compos*. 2004;33(5):189-194.
<http://dx.doi.org/10.1179/174328904x4864>
- [9] Hine PJ, Ward IM, Teckoe J. The hot compaction of woven polypropylene tapes. *Journal of Materials Science*. 1998;33(11):2725-2733.
<http://dx.doi.org/10.1023/A:1017540530295>
- [10] Hine PJ, Unwin AP, Ward IM. The use of an interleaved film for optimising the properties of hot compacted polyethylene single polymer composites. *Polymer*. 2011;52(13):2891-2898.
<http://dx.doi.org/10.1016/j.polymer.2011.04.026>
- [11] Ward IM, Hine PJ. Novel composites by hot compaction of fibers. *Polymer Engineering and Science*. 1997;37(11):1809-1814.
- [12] Barkoula NM, Alcock B, Cabrera NO, Peijs T. Fatigue properties of highly oriented polypropylene tapes and all-polypropylene composites. *Polym Polym Compos*. 2008;16(2):101-113.
- [13] Alcock B, Cabrera NO, Barkoula NM, Loos J, Peijs T. Interfacial properties of highly oriented coextruded polypropylene tapes for the creation of recyclable all-polypropylene composites. *Journal of Applied Polymer Science*. 2007;104(1):118-129.
<http://dx.doi.org/10.1002/app.24588>
- [14] Alcock B, Cabrera NO, Barkoula NM, Peijs T. The effect of processing conditions on the mechanical properties and thermal stability of highly oriented PP tapes. *European Polymer Journal*. 2009;45(10):2878-2894.
<http://dx.doi.org/10.1016/j.eurpolymj.2009.06.025>
- [15] Houshyar S, Shanks RA. Mechanical and thermal properties of toughened polypropylene composites. *Journal of Applied Polymer Science*. 2007;105(2):390-397.
<http://dx.doi.org/10.1002/app.25034>
- [16] Bárány T, Izer A, Karger-Kocsis J. Impact resistance of all-polypropylene composites composed of alpha and beta modifications. *Polym Test*. 2009;28:176-182.
<http://dx.doi.org/10.1016/j.polymertesting.2008.11.011>
- [17] Chen JC, Wu CM, Pu FC, Chiu CH. Fabrication and mechanical properties of self-reinforced poly(ethylene terephthalate) composites. *Express Polymer Letters*. 2011;5(3):288-237.
<http://dx.doi.org/10.3144/expresspolymlett.2011.22>

- [18] Pegoretti A, ZA, Migliaresi C. Preparation and tensile mechanical properties of unidirectional liquid crystalline single-polymer composites. *Composites Science and Technology*. 2006;66:1970-1979.
<http://dx.doi.org/10.1016/j.compscitech.2006.01.012>
- [19] Izer A, Bárány T. Effect of consolidation on the flexural creep behaviour of all-polypropylene composite. *Express Polymer Letters*. 2010;4(4):210-216.
<http://dx.doi.org/10.3144/expresspolymlett.2010.27>
- [20] Houshyar S, Shanks RA, Hodzic A. Influence of different woven geometry in poly(propylene) woven composites. *Macromol Mater Eng*. 2005;290(1):45-52.
<http://dx.doi.org/10.1002/mame.200400158>
- [21] Matabola KP, de Vries AR, Luyt AS, Kumar R. Studies on single polymer composites of poly(methyl methacrylate) reinforced with electrospun nanofibers with a focus on their dynamic mechanical properties. *Express Polymer Letters*. 2011;5(7):635-642.
<http://dx.doi.org/10.3144/expresspolymlett.2011.61>
- [22] Izer A, Bárány T, Varga J. Development of woven fabric reinforced all-polypropylene composites with beta nucleated homo- and copolymer matrices. *Composites Science and Technology*. 2009;69(13):2185-2192.
<http://dx.doi.org/10.1016/j.compscitech.2009.06.002>
- [23] Bárány T, Izer A, Czigány T. On consolidation of self-reinforced polypropylene composites. *Plast Rubber Compos*. 2006;35(9):375-379.
<http://dx.doi.org/10.1179/174328906X128234>
- [24] Karian HG. Part shrinkage behavior of polypropylene resins and polypropylene composites. In: Karian HG, editor. *Handbook of Polypropylene and Polypropylene composites*. Second ed, vol. 19 New York: Marcel Dekker; 2003. p. 675-706.
- [25] Sikló B, Cameron K, Kovács JG. Deformation analysis of short glass fiber-reinforced polypropylene injection-molded plastic parts. *J Reinf Plast Compos*. 2011;30(16):1367-1372.
<http://dx.doi.org/10.1177/0731684411426203>
- [26] Kovács JG. Shrinkage Alteration Induced by Segregation of Glass Beads in Injection Molded PA6: Experimental Analysis and Modeling. *Polymer Engineering and Science*. 2011;51(12):2517-2525.
<http://dx.doi.org/10.1002/pen.22025>
- [27] Kovács JG, Solymossy B. Effect of Glass Bead Content and Diameter on Shrinkage and Warpage of Injection-Molded PA6. *Polymer Engineering and Science*. 2009;49(11):2218-2224.
<http://dx.doi.org/10.1002/pen.21470>
- [28] Karger Kocsis J. Processing and properties of reinforced polypropylenes. In: Karger Kocsis J, editor. *Polypropylene Structure, blends and composites*, vol. 3 Cambridge: Chapman&Hall; 1995. p. 71-112.
- [29] Ehrenstein GW. Overview of Selected Polymeric Materials. *Polymeric Materials*, Vol. 1 Munich: Hanser; 2001. p. 253.
- [30] Karger-Kocsis J, Wanjale SD, Abraham T, Bárány T, Apostolov AA. Preparation and characterization of polypropylene homocomposites: Exploiting polymorphism of PP homopolymer. *Journal of Applied Polymer Science*. 2010;115(2):684-691.
<http://dx.doi.org/10.1002/app.30624>

[31] Karger-Kocsis J, Friedrich K. Temperature and strain rate effects on the fracture toughness of PEEK and its short glass fibre reinforced composite. *Polymer*. 1986;27(11):1753-1760.

[32] Gibson AG. Processing and properties of reinforced polypropylenes. In: Karger Kocsis J, editor. *Polypropylene*, vol. 3 Cambridge: Chapman&Hall; 1995. p. 82-90.

Lists of the figures:

Figure 1 DSC curves of the matrix (a) and the reinforcement (b)

Figure 2 FTIR spectra of random polypropylene copolymer and thermoplastic elastomer

Figure 3 Preparation of unidirectional all-PP composites by filament winding (a) followed by compression moulding (b)

Figure 4 SEM picture of the cross section of the consolidated sheet

Figure 5 Injection moulded plaque specimen and the measuring positions for shrinkage. Designations: LM – length dimension at the middle; LS – length dimension at the side; WE – width dimension at the front; WB – width dimension at the back

Figure 6 Preparation of the dumbbell specimens from the plaque specimens in parallel and perpendicular to the flow direction and position of the analyzed cross section by LM

Figure 7 Shrinkage of the all-PP composites at different processing temperature

Figure 8 DMA traces of the all-PP composites (C) and TPE matrix (M) material injection moulded at different temperatures (120, 140, 160°C)

Figure 9 Yield stress (a) and tensile modulus (b) of the TPE matrix and all-PP composites produced by injection and compression moulding at 140°C

Figure 10 Force-time curves registered in IFWI testing at room temperature (RT) and -30°C for the matrix (M) and all-PP composite (C) injection moulded at 120°C

Figure 11 Cross sections of the all-PP composites in flow direction (SIDE) Designations: processing (melt) temperatures: a) 120°C; b) 140°C; c) 160°C

Figure 12 Cross sections of the all-PP composite perpendicular to the flow direction in the front region as a function of the processing temperature. Designations: melt temperatures: a) 120°C; b) 140°C; c) 160°C (Red arrows designate the flow direction)

Figure 13 Fracture surfaces of the all-PP composites injection moulded at a) 120°C; b) 140°C; c) 160°C, respectively

Figure 14 SEM pictures demonstrating the fibre/matrix adhesion on fracture surfaces of all-PP composites injection moulded at a) 120°C; b) 140°C; c) 160°C, respectively

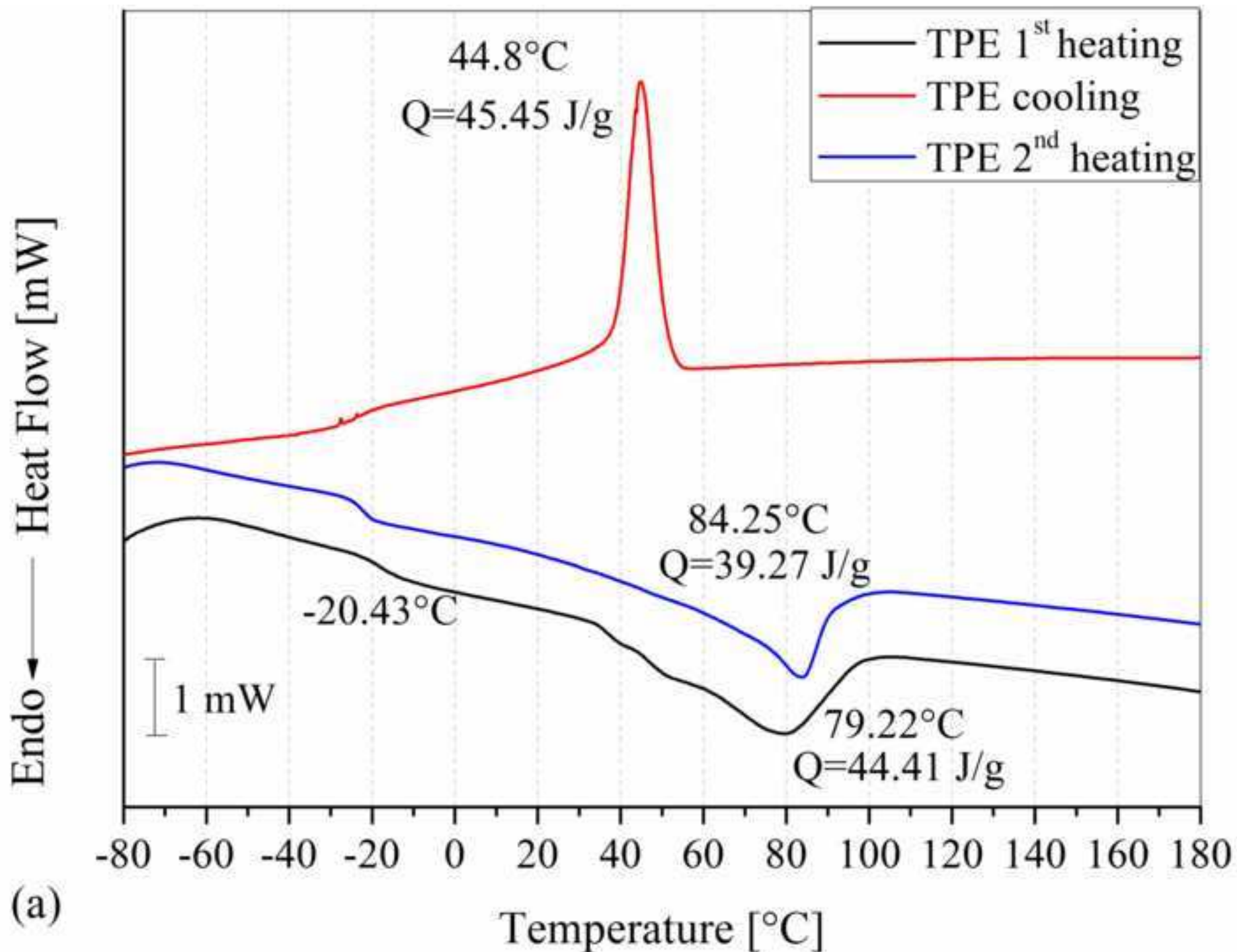
Lists of the tables:

Table 1 Yield stress, tensile modulus and perforation energy of the matrix and all-PP composites as a function of processing (melt) temperature and specimen cut-off

Temperature [°C]	SECTION	Yield stress [MPa]		Tensile Modulus [MPa]		Perforation energy (RT) [J/mm]		Perforation energy (-30°C) [J/mm]	
		Matrix	Composite	Matrix	Composite	Matrix	Composite	Matrix	Composite
120	SIDE	6.6±0.3	20.5±1.3	74.4±14.4	781.4±87.7				
	MIDDLE	6.5±0.2	13.6±0.1	63.3±4.4	623.2±43.7				
	FRONT	6.9±0.1	17.2±2.7	106.4±22.1	695.8±170.3	17.0±0.3	6.8±0.4	27.2±0.7	7.3±0.8
	CENTER	6.8±0.0	24.0±7.1	114.2±2.4	870.4±103.3				
	BACK	6.5±0.0	31.0±5.4	101.1±5.1	1029.2±68.1				
140	SIDE	6.9±0.1	20.3±4.1	82.4±2.6	734.3±78.6				
	MIDDLE	6.6±0.1	13.6±1.2	68.4±10.5	650.7±33.5				
	FRONT	7.3±0.1	23.2±1.8	142.0±5.3	558.7±123.5	13.6±0.3	7.8±0.2	25.3±0.8	6.9±0.9
	CENTER	6.9±0.1	27.9±3.9	134.9±0.3	811.4±67.9				
	BACK	6.7±0.3	34.2±3.9	124.5±5.6	912.4±40.4				
160	SIDE	6.4±0.3	29.6±0.5	84.5±4.2	748.6±4.8				
	MIDDLE	6.2±0.2	18.2±0.7	79.5±7.8	619.9±34.6				
	FRONT	7.4±0.1	22.8±1.1	148.4±1.5	734.9±145.4	15.7±0.3	9.5±1	27.7±0.6	5.3±0.5
	CENTER	7.1±0.0	27.1±1.4	138.0±2.0	777.7±167.0				
	BACK	6.6±0.5	35.6±2.8	119.5±8.4	872.0±20.1				

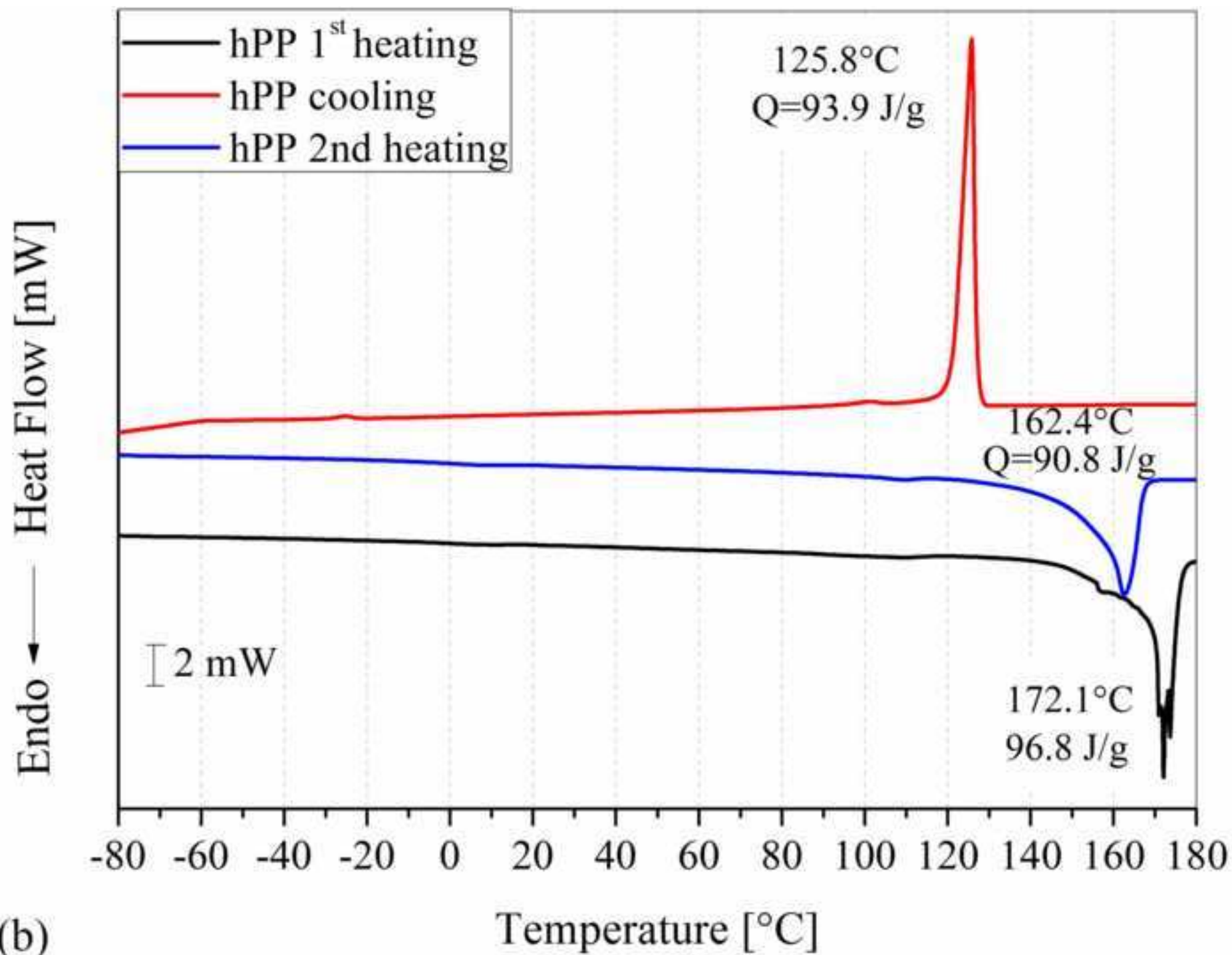
Table 1 Yield stress, tensile modulus and perforation energy of the matrix and all-PP composites as a function of processing (melt) temperature and specimen cut-off

Figure_1_a
[Click here to download high resolution image](#)



(a)

Figure_1_b
[Click here to download high resolution image](#)



(b)

Figure_2
[Click here to download high resolution image](#)

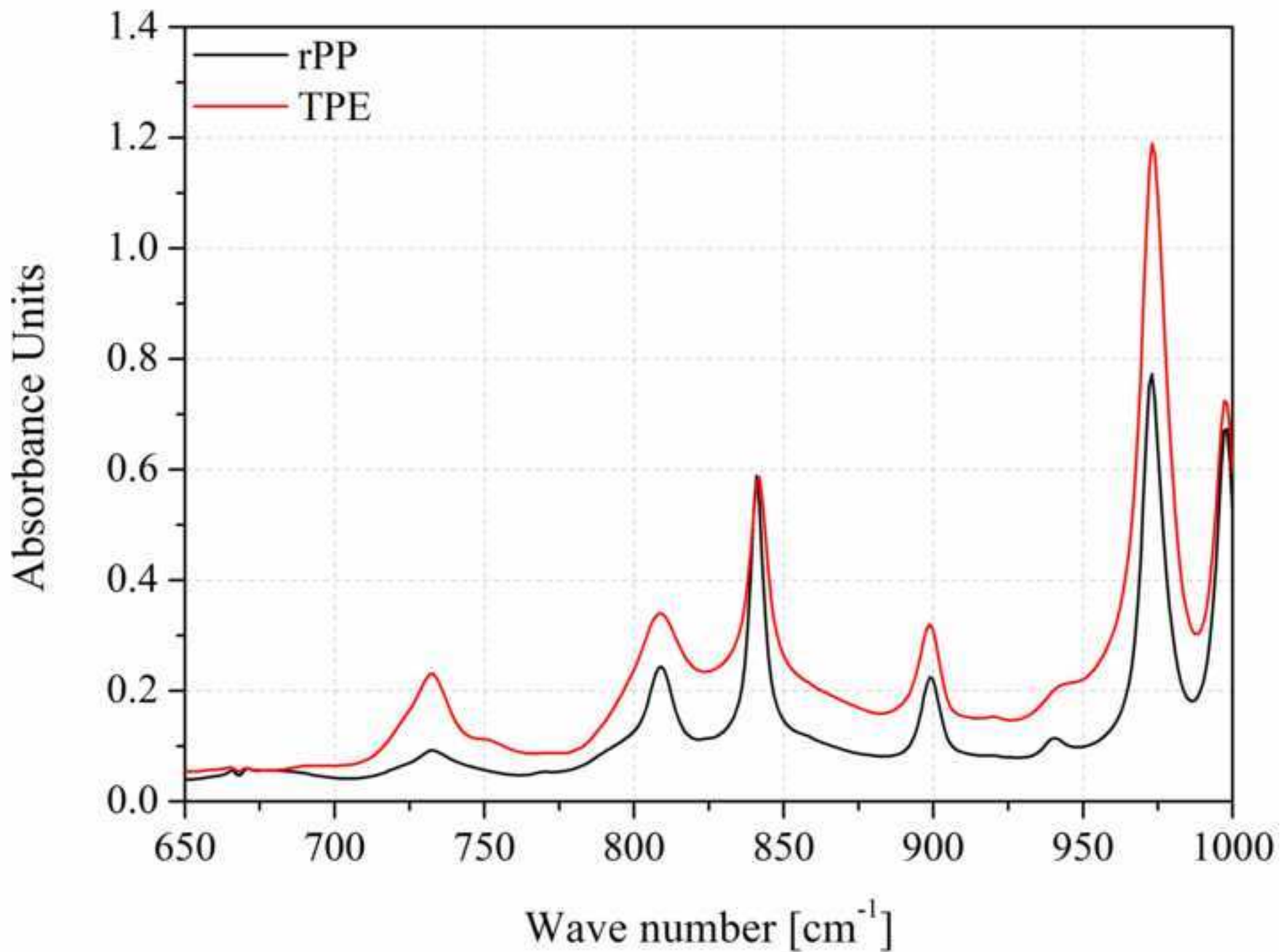


Figure_3

[Click here to download high resolution image](#)

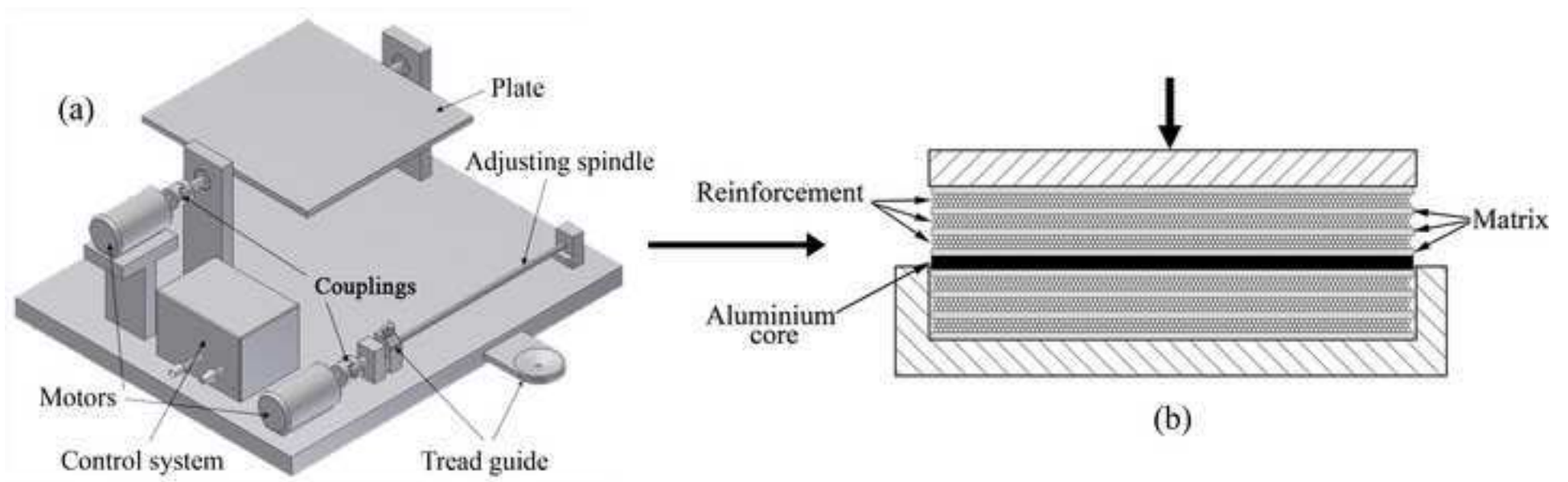
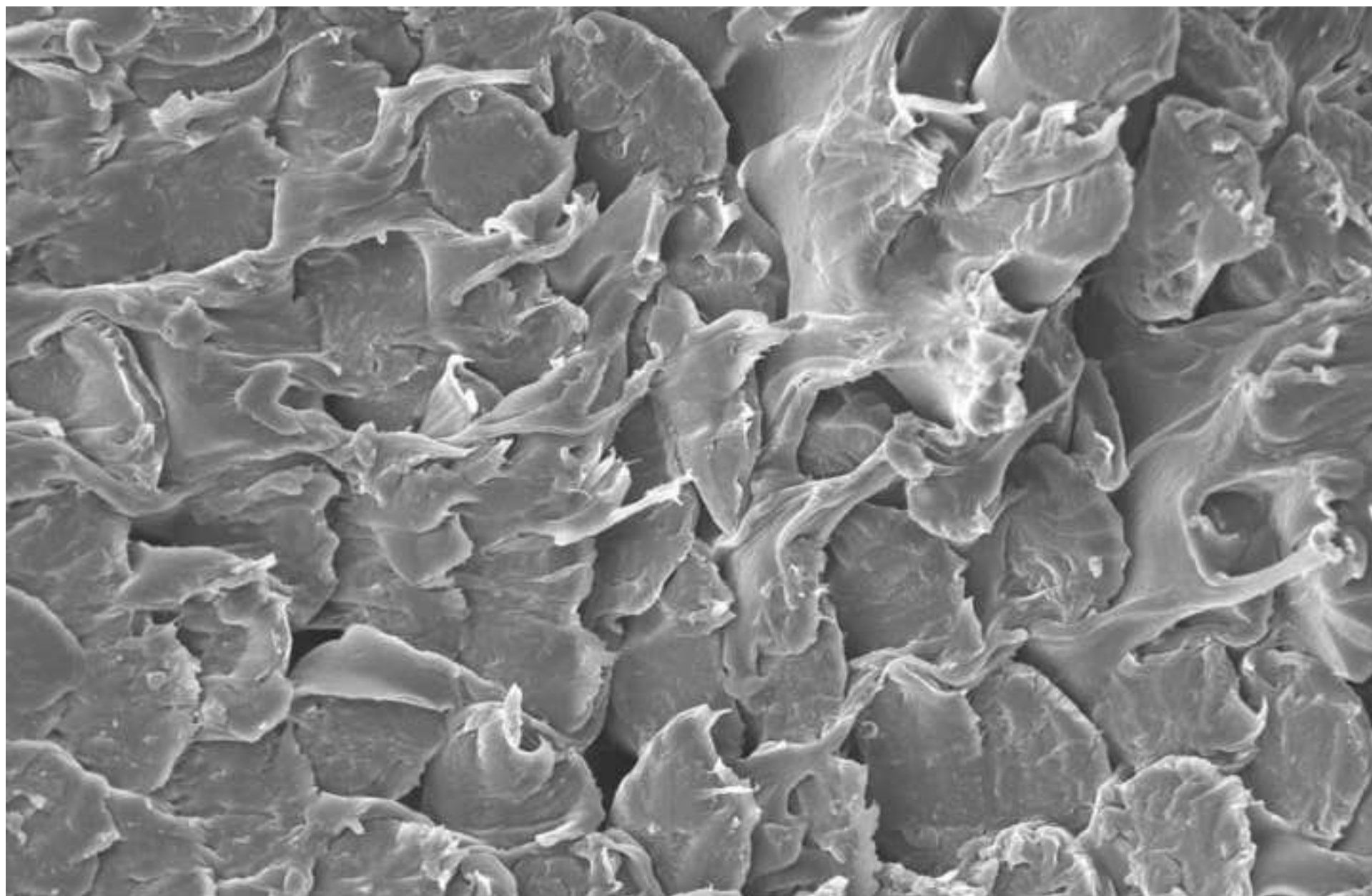


Figure_4
[Click here to download high resolution image](#)



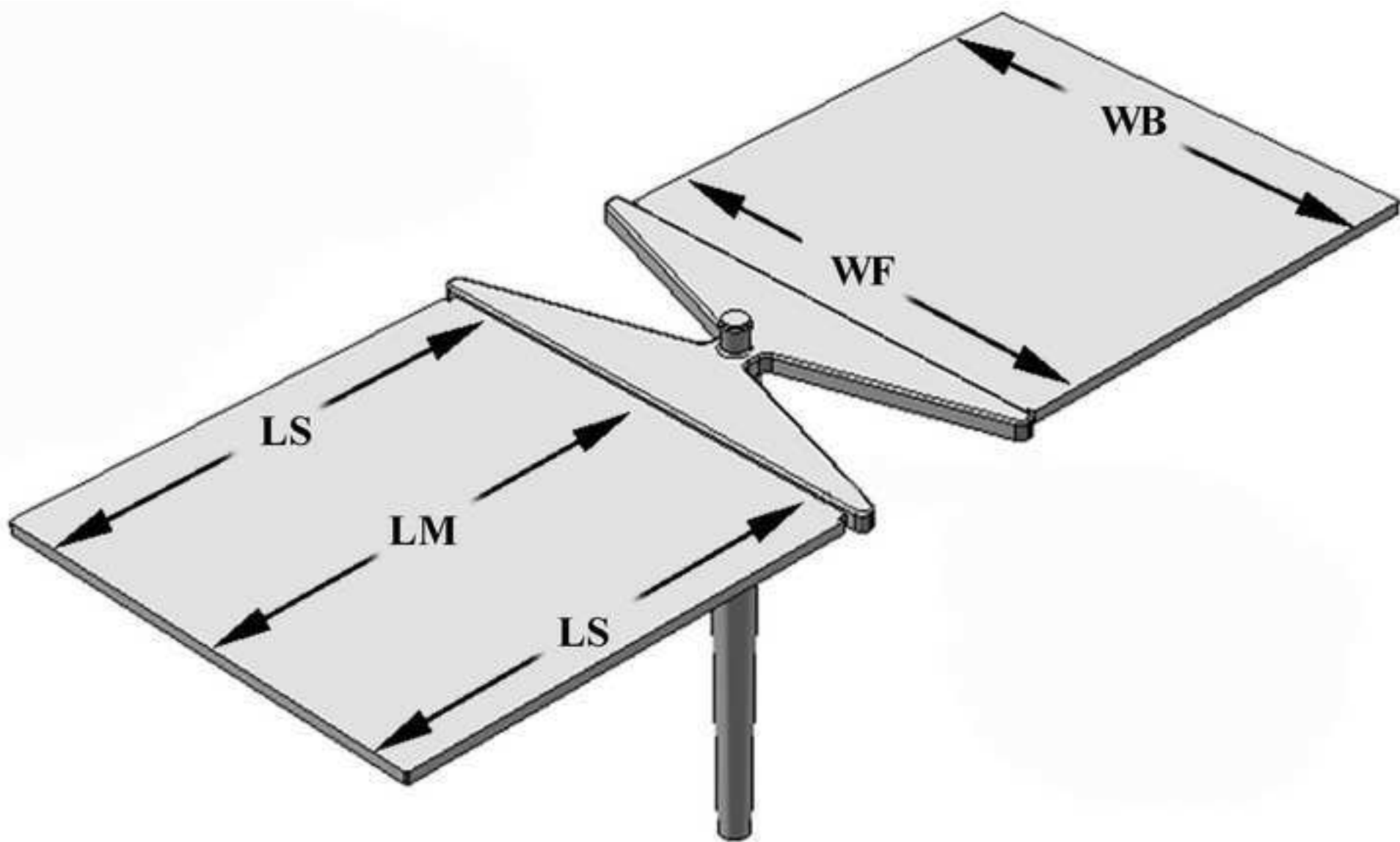
15kV

X300

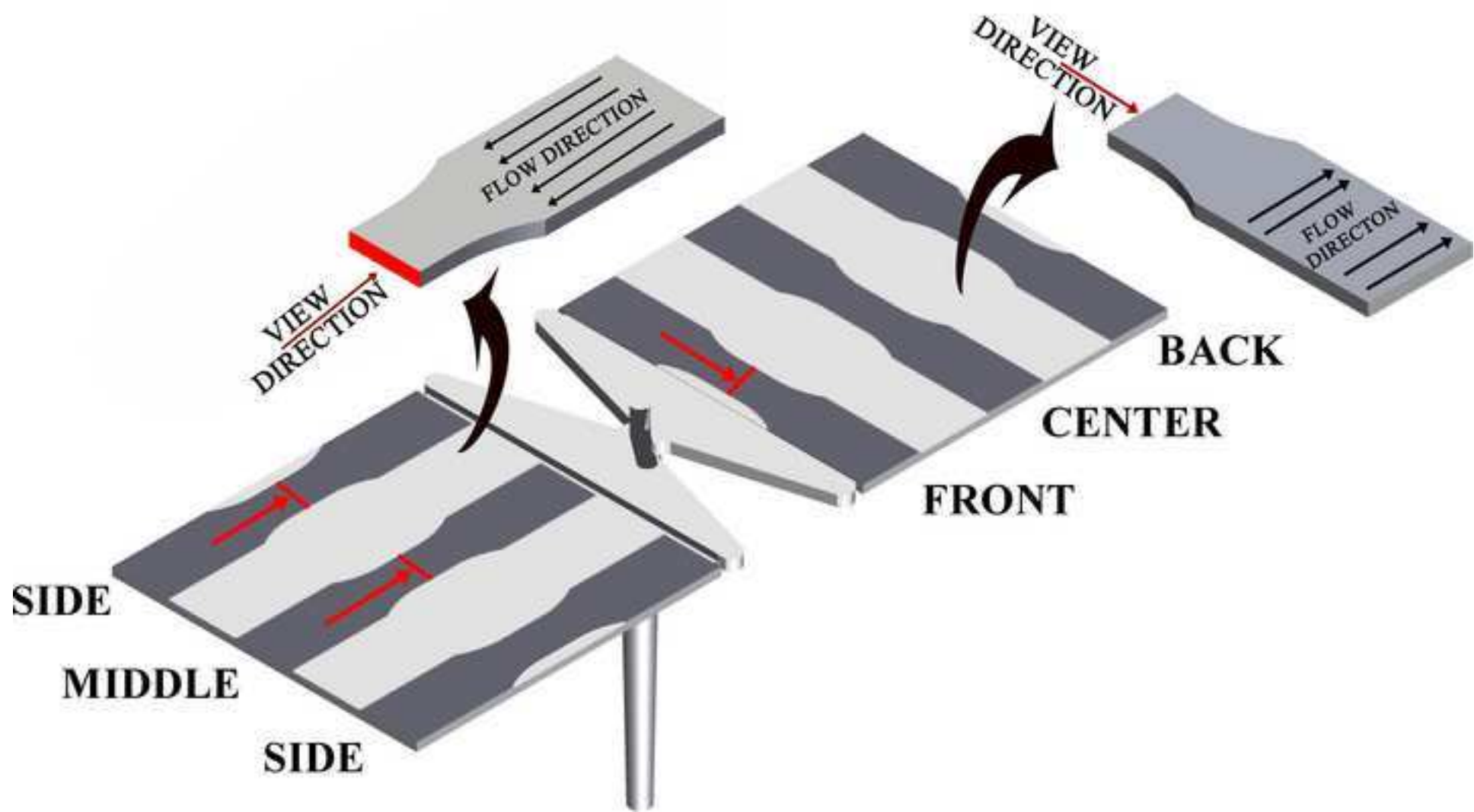
50 μ m

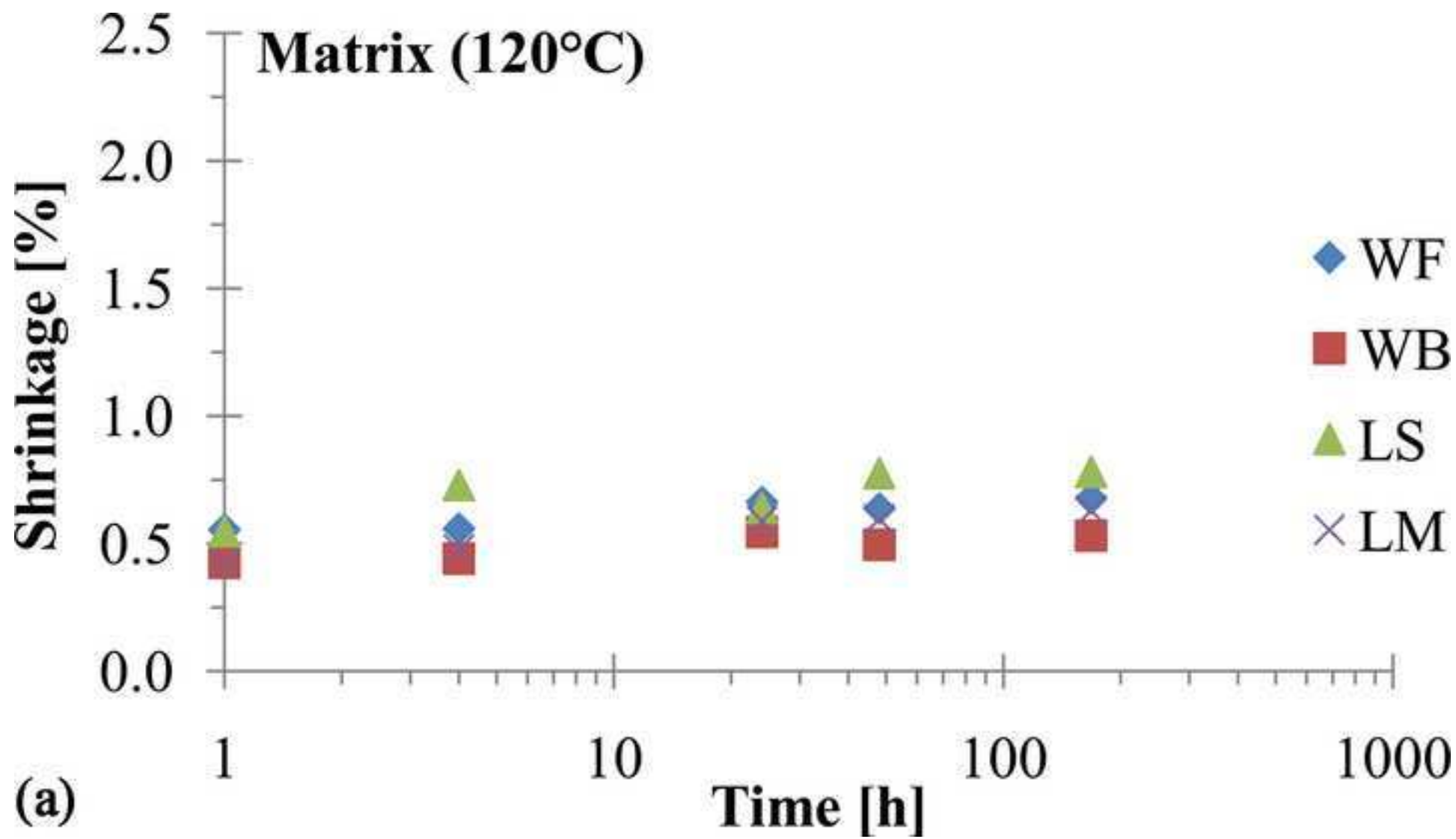
11 50 SEI

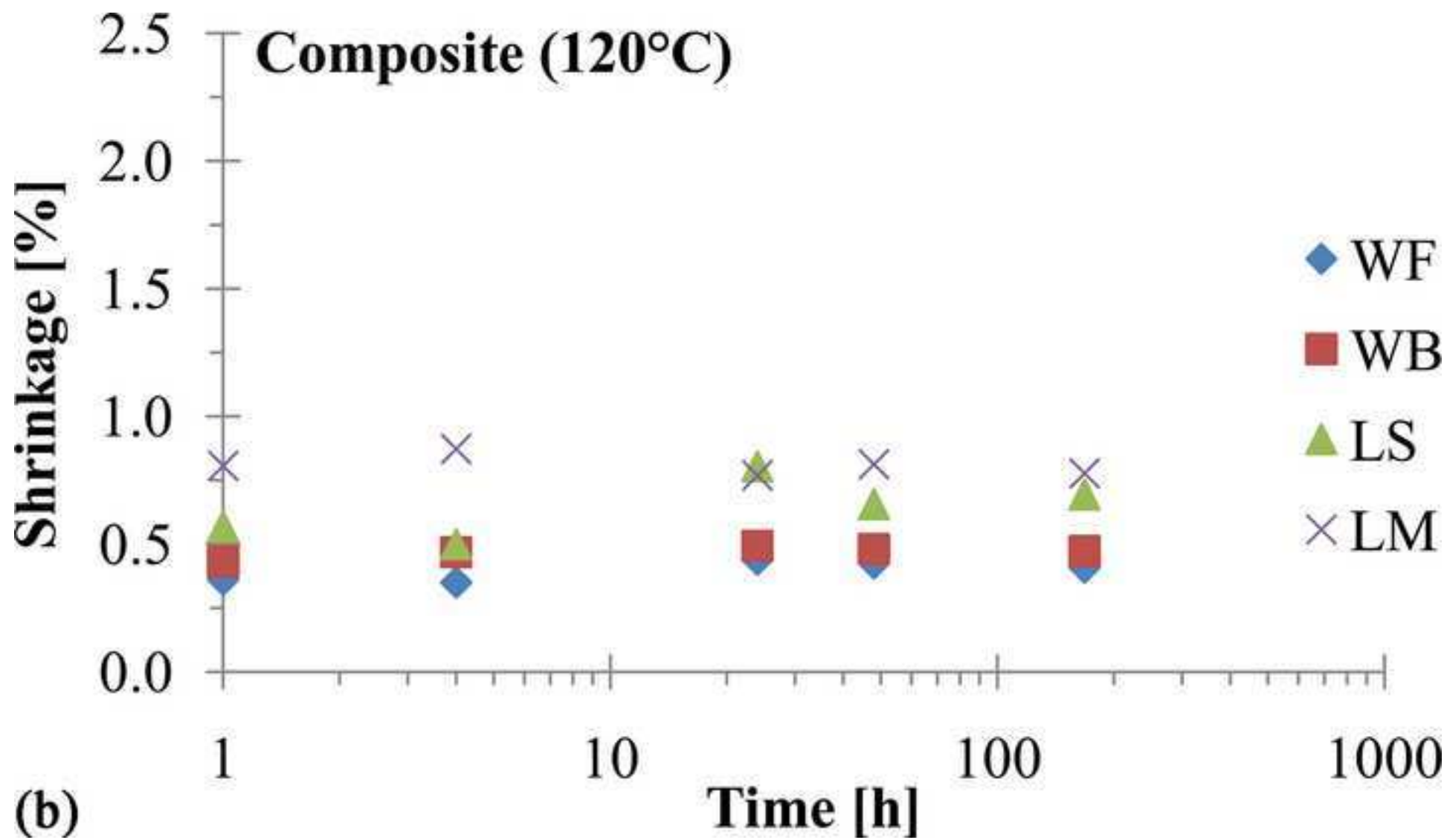
Figure_5
[Click here to download high resolution image](#)



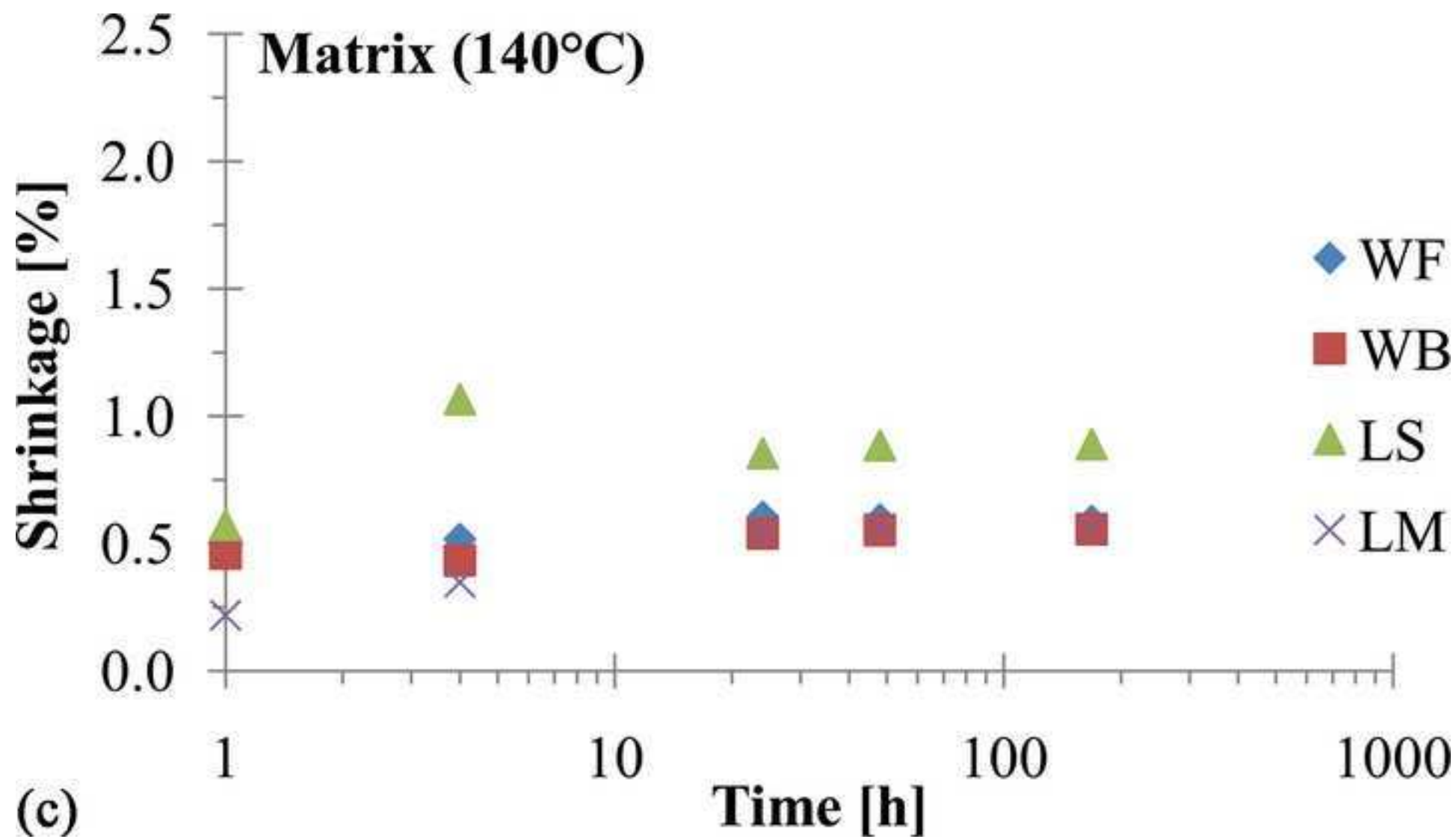
Figure_6
[Click here to download high resolution image](#)

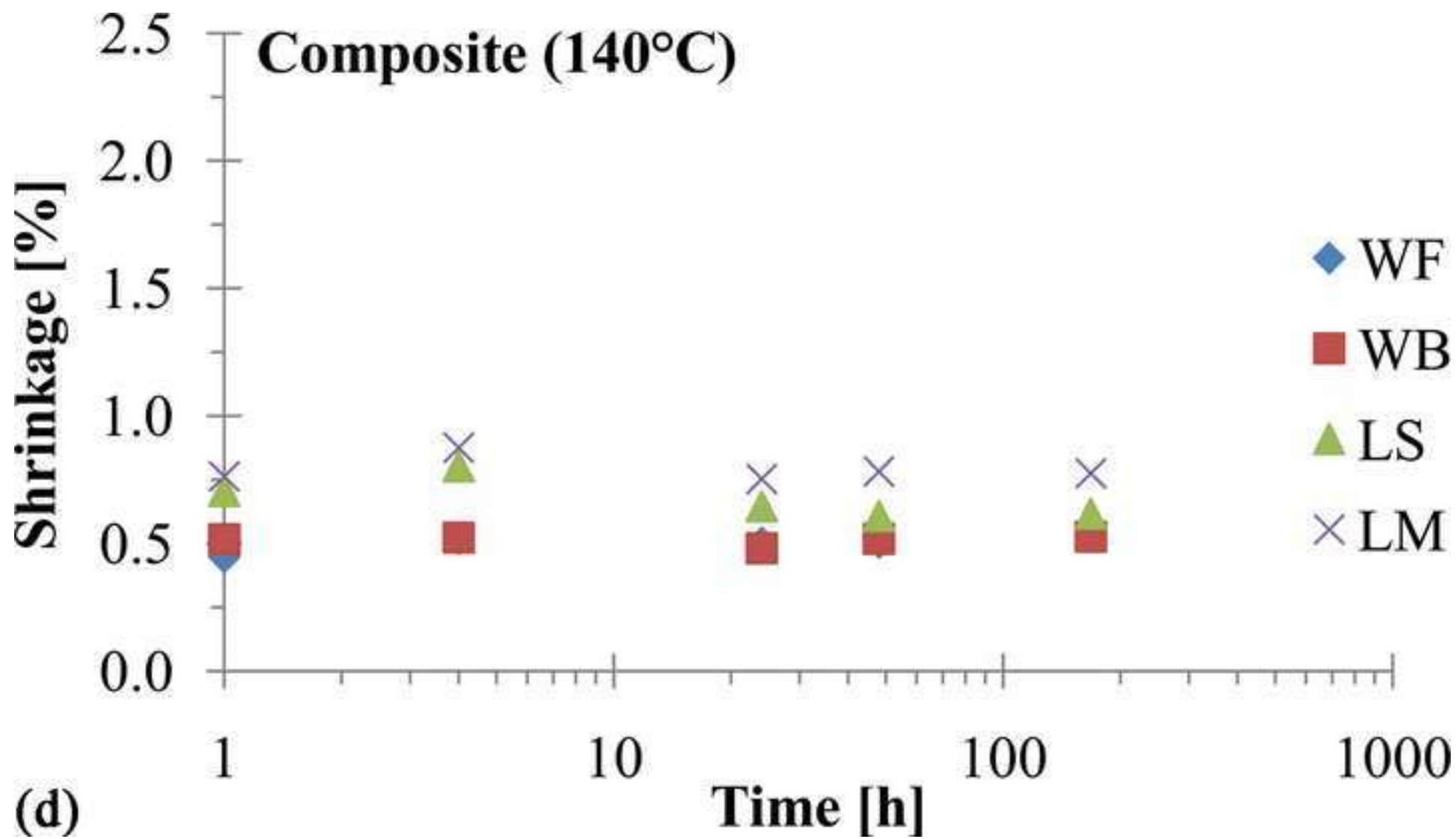


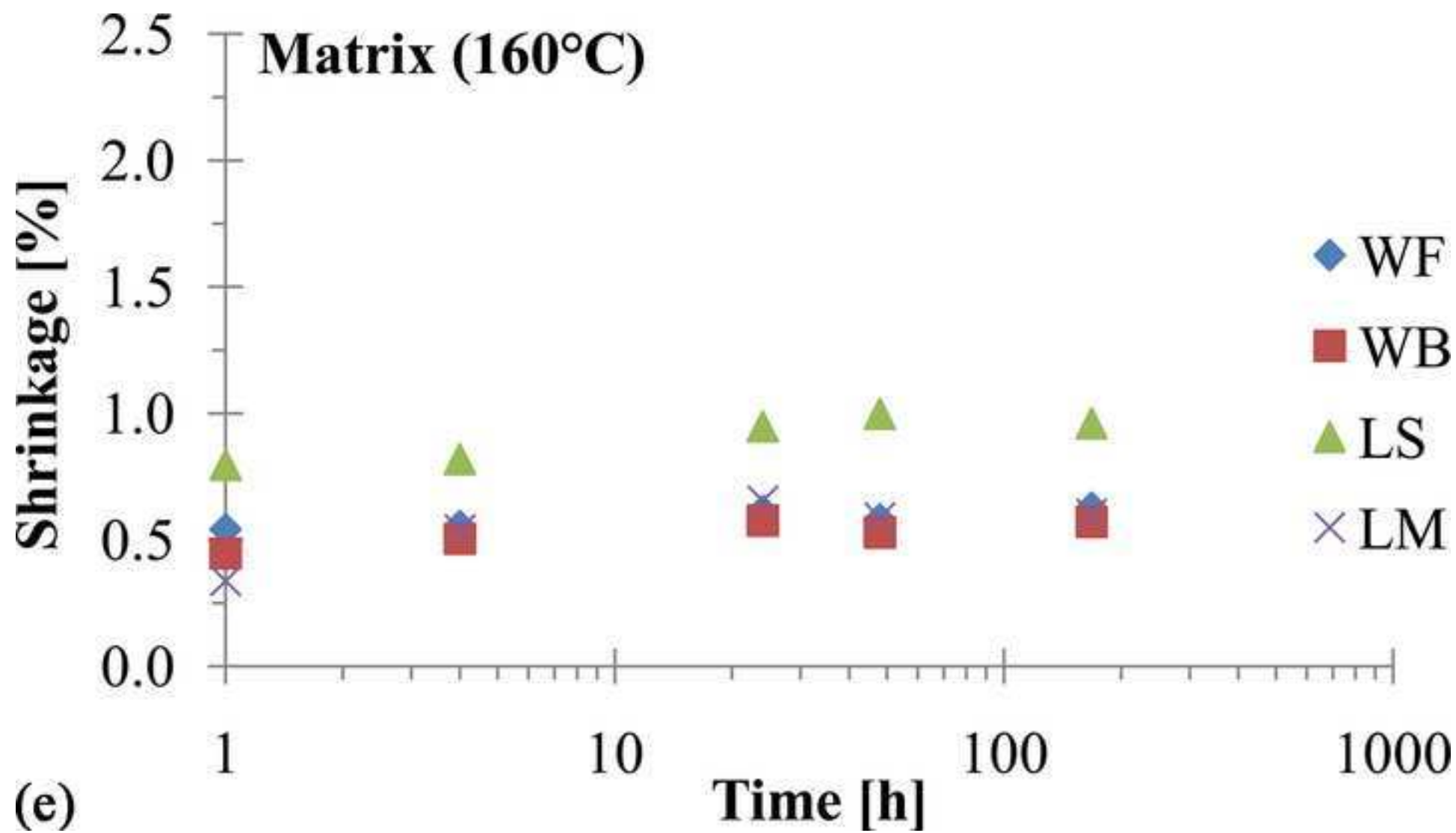




(b)







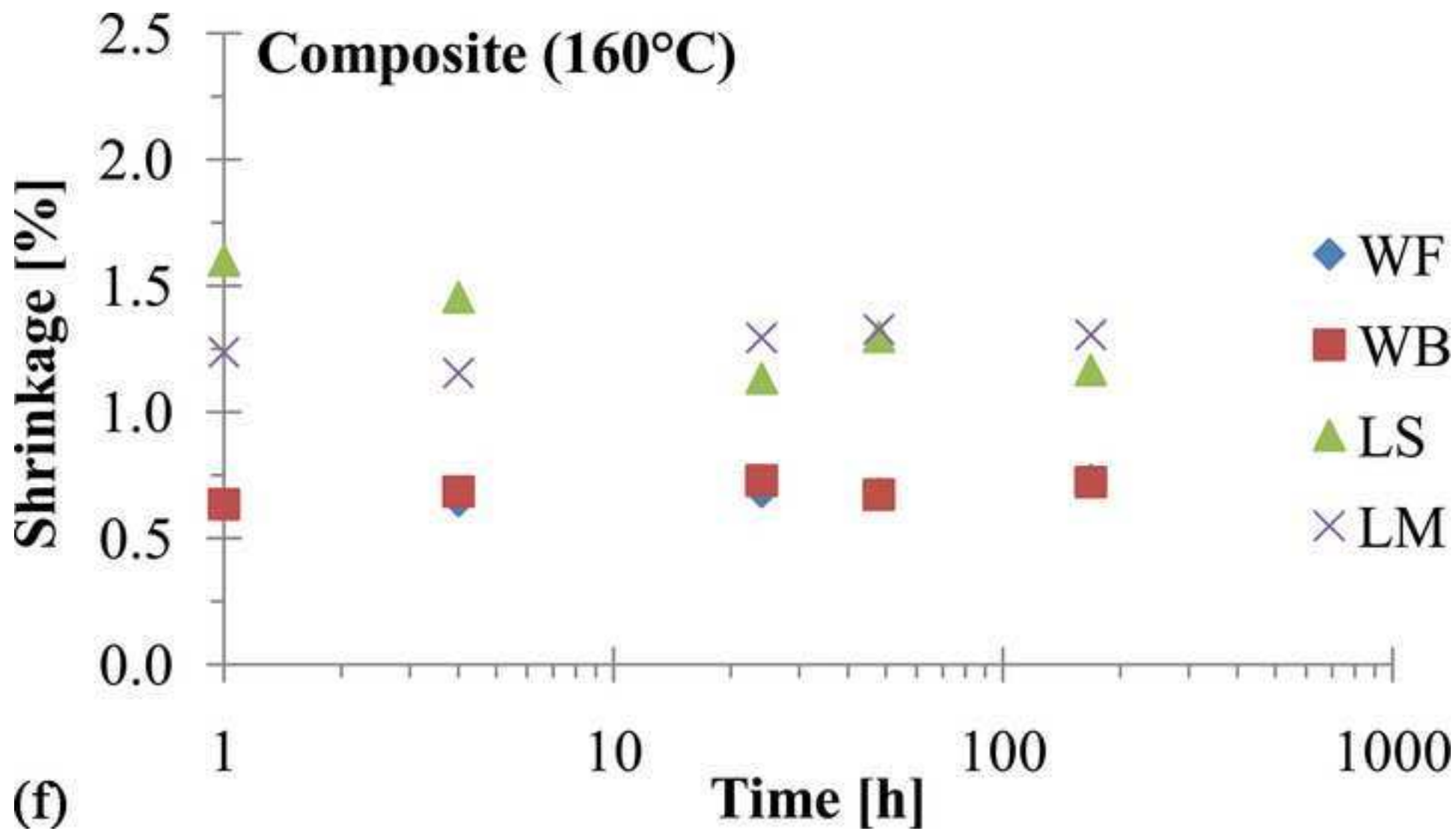
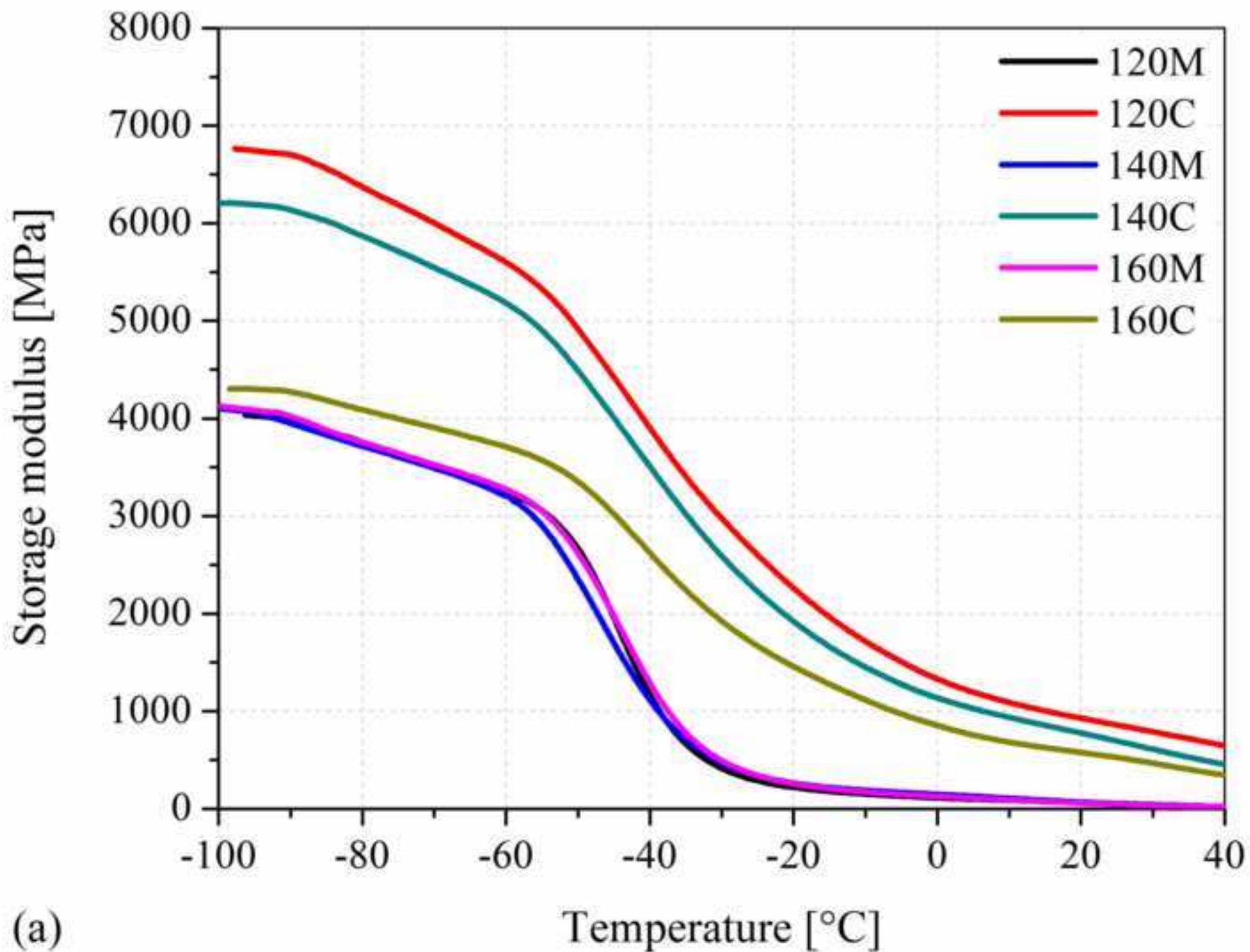
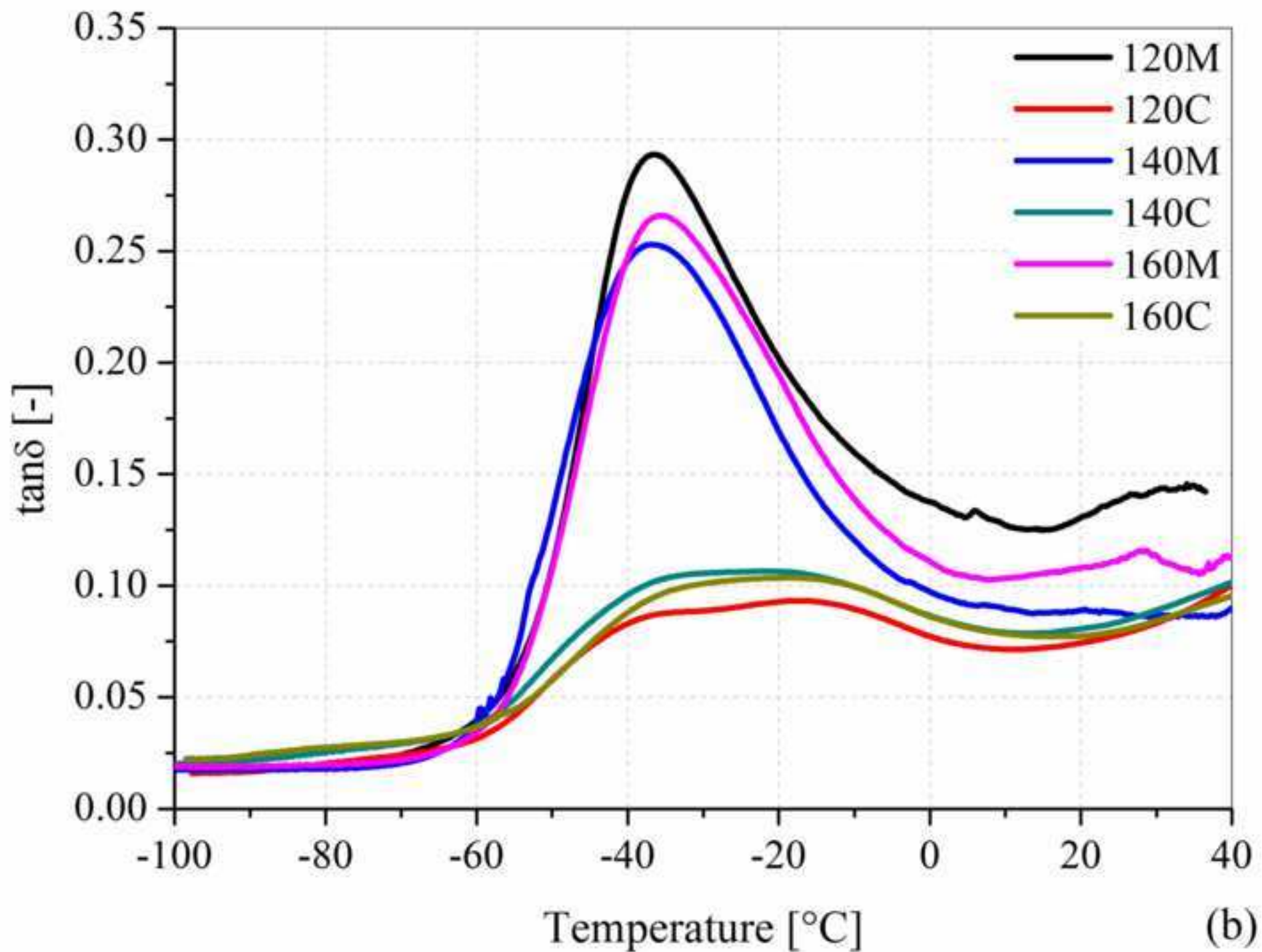


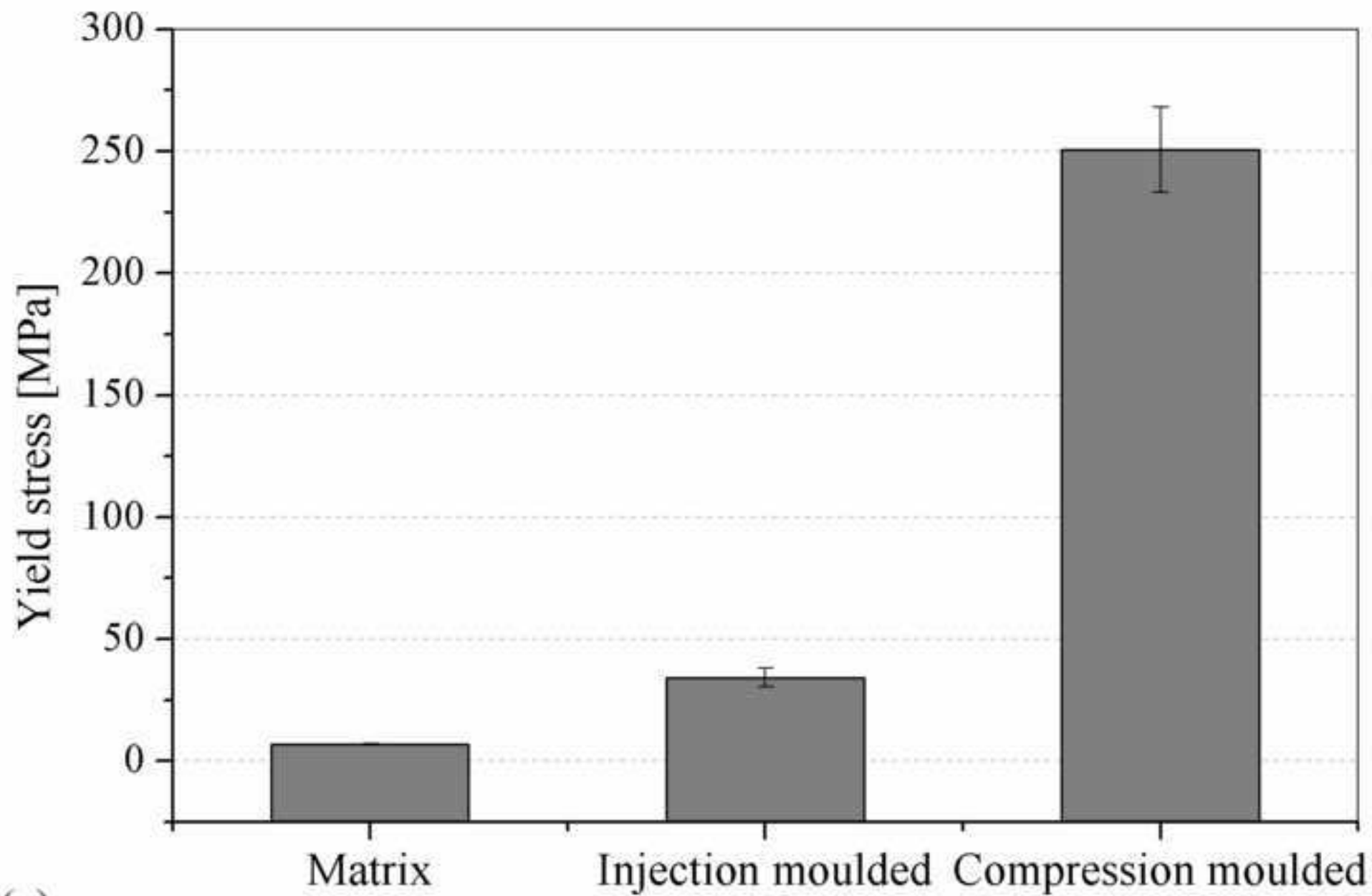
Figure_8_a
[Click here to download high resolution image](#)



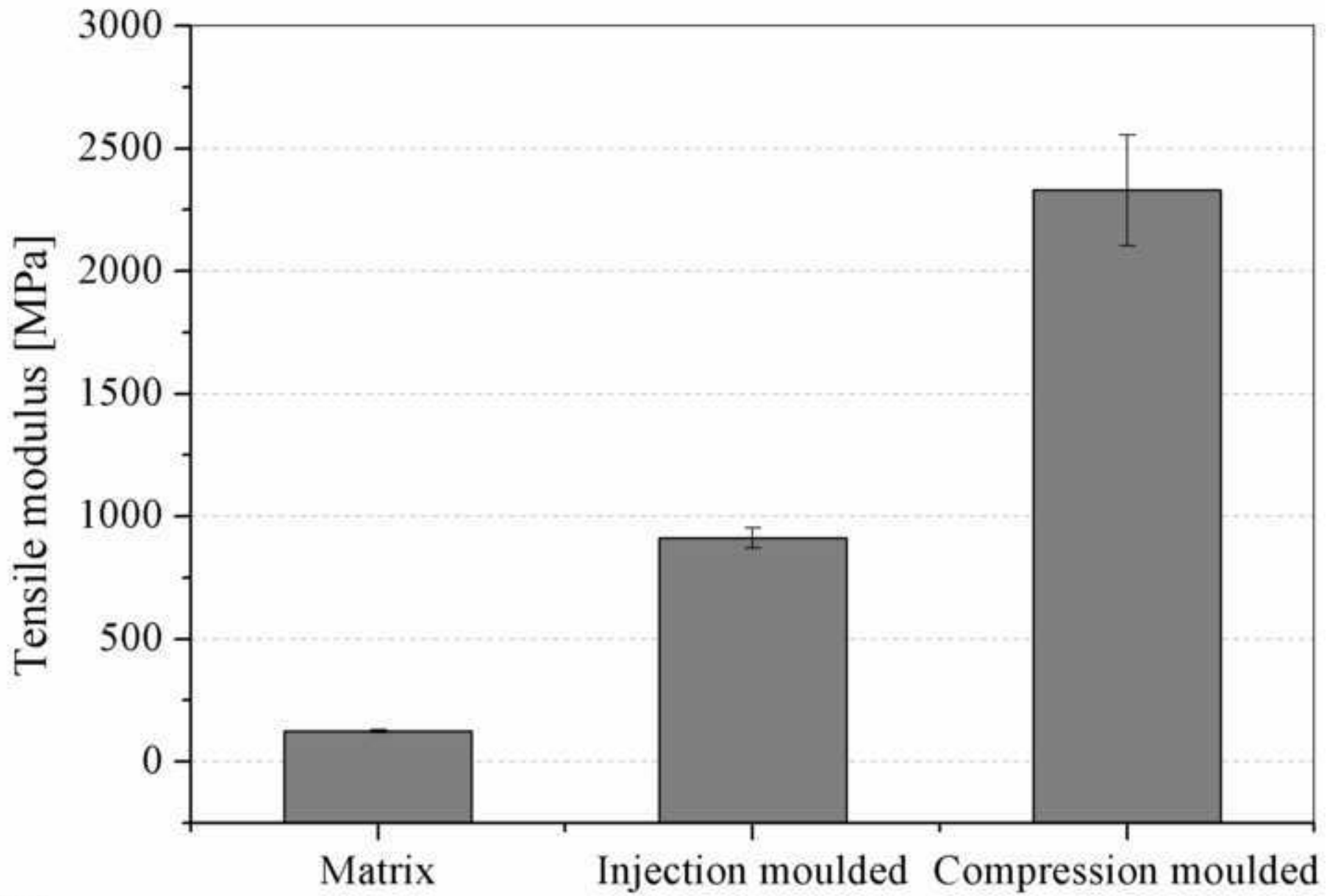
(a)

Figure_8_b
[Click here to download high resolution image](#)





(a)



(b)

Figure_10
[Click here to download high resolution image](#)

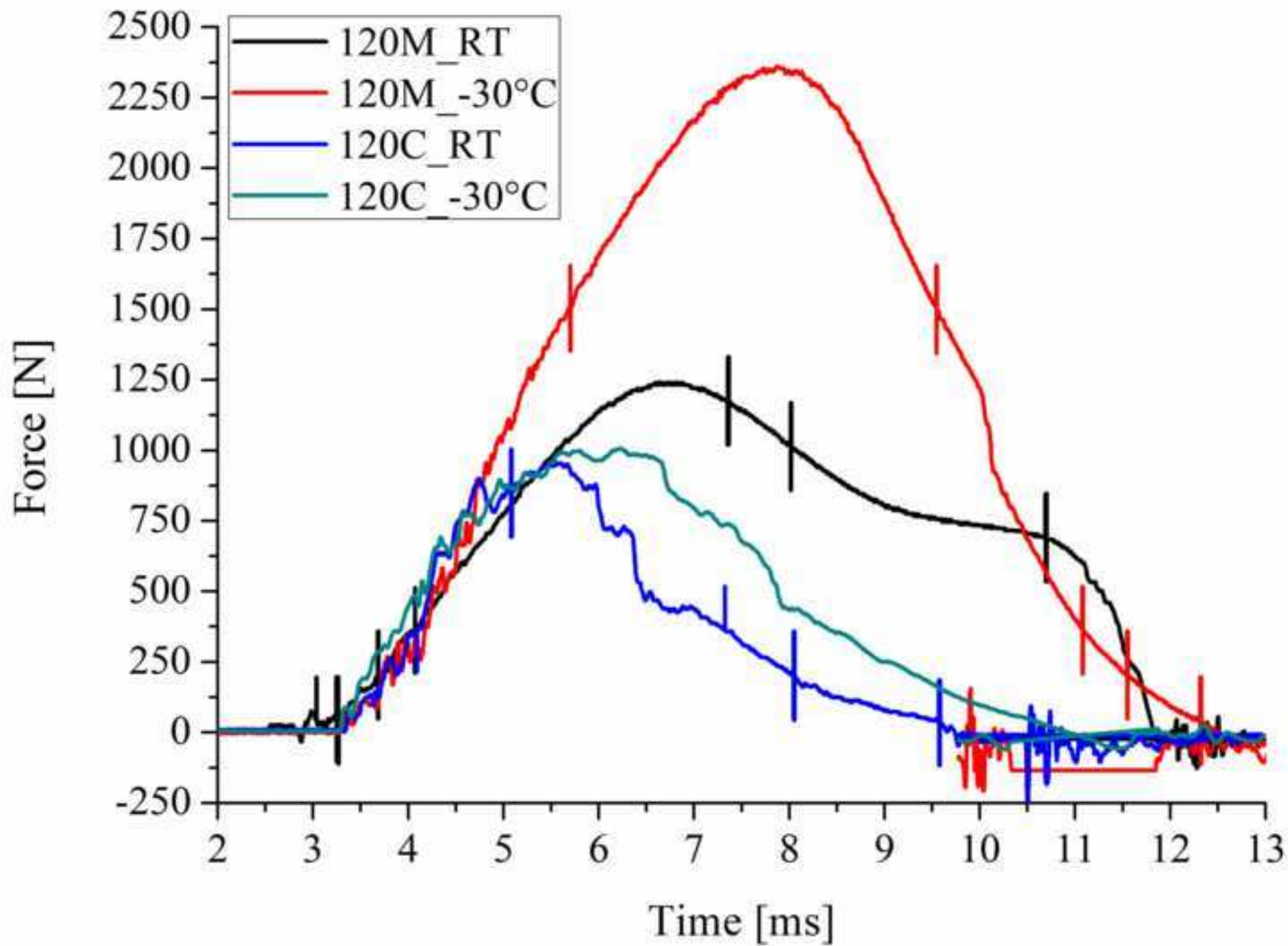


Figure_11
[Click here to download high resolution image](#)

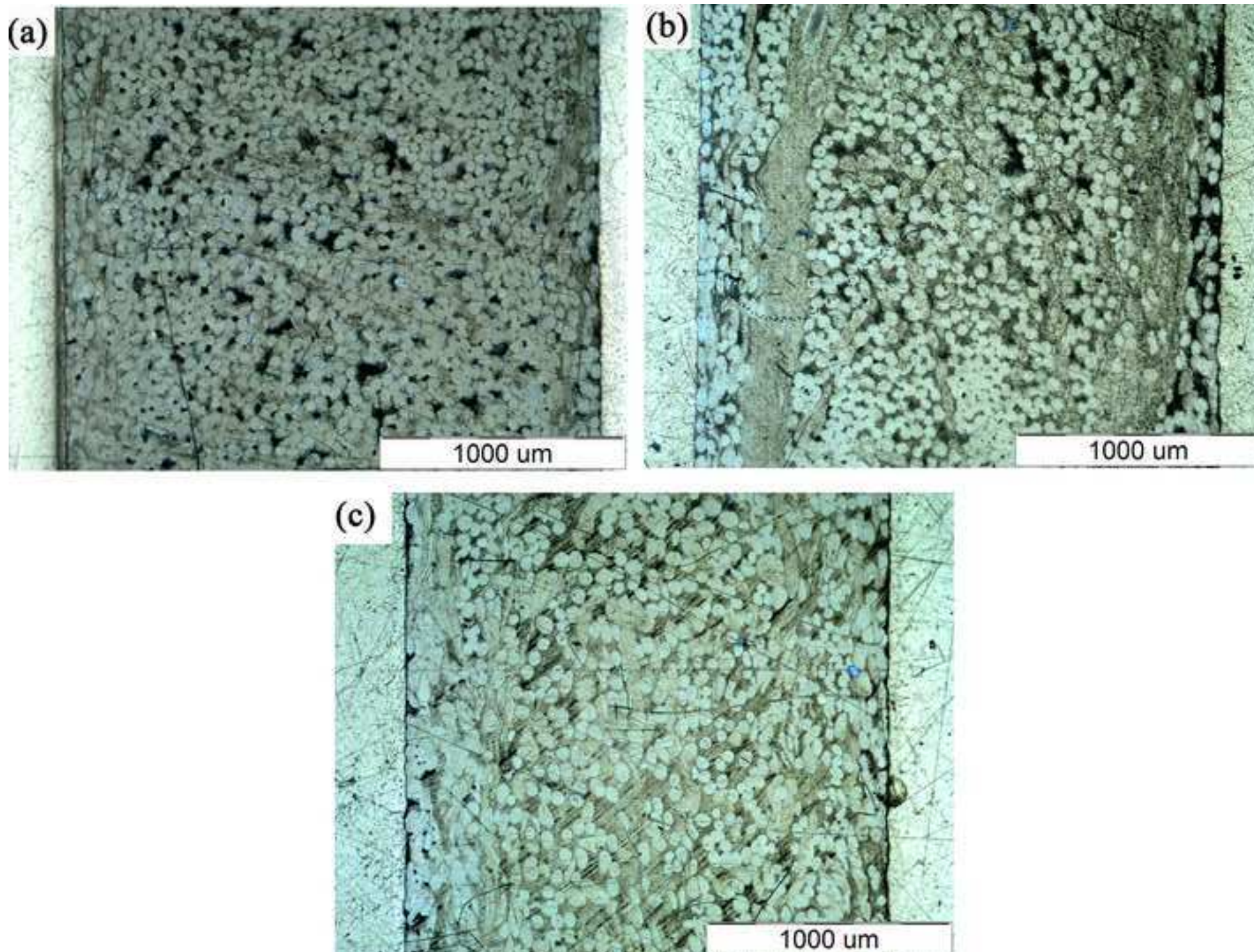


Figure_12
[Click here to download high resolution image](#)

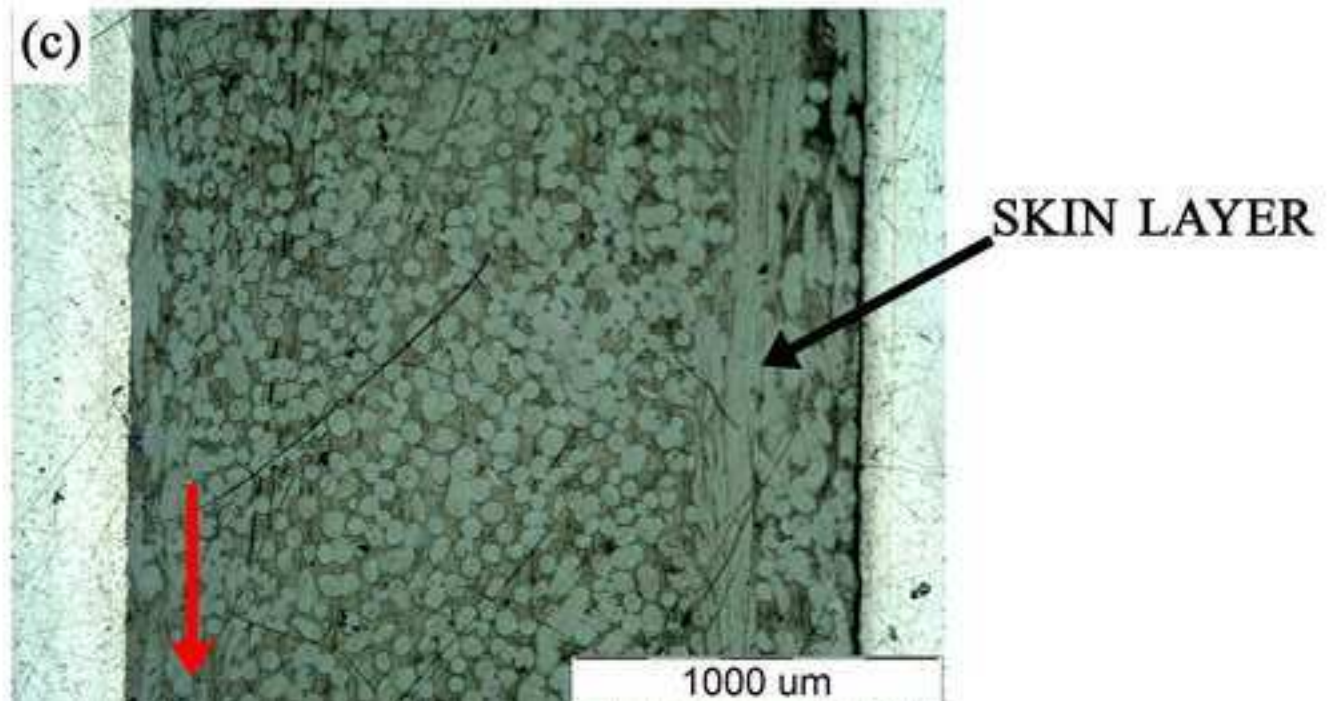
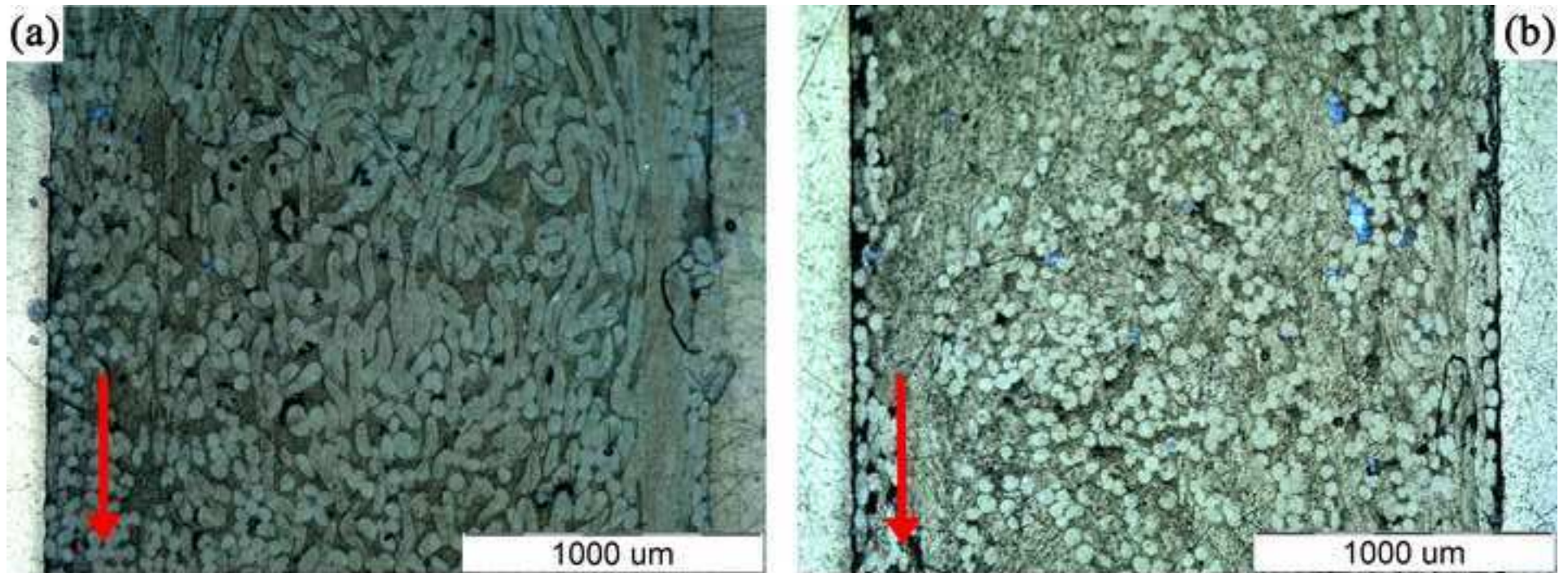


Figure_13
[Click here to download high resolution image](#)

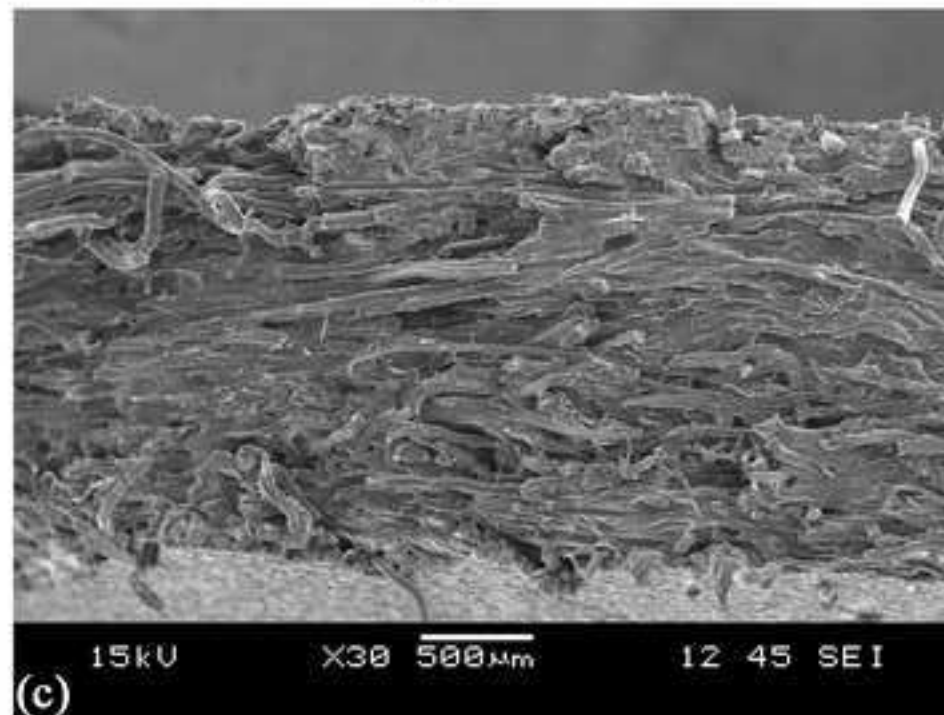
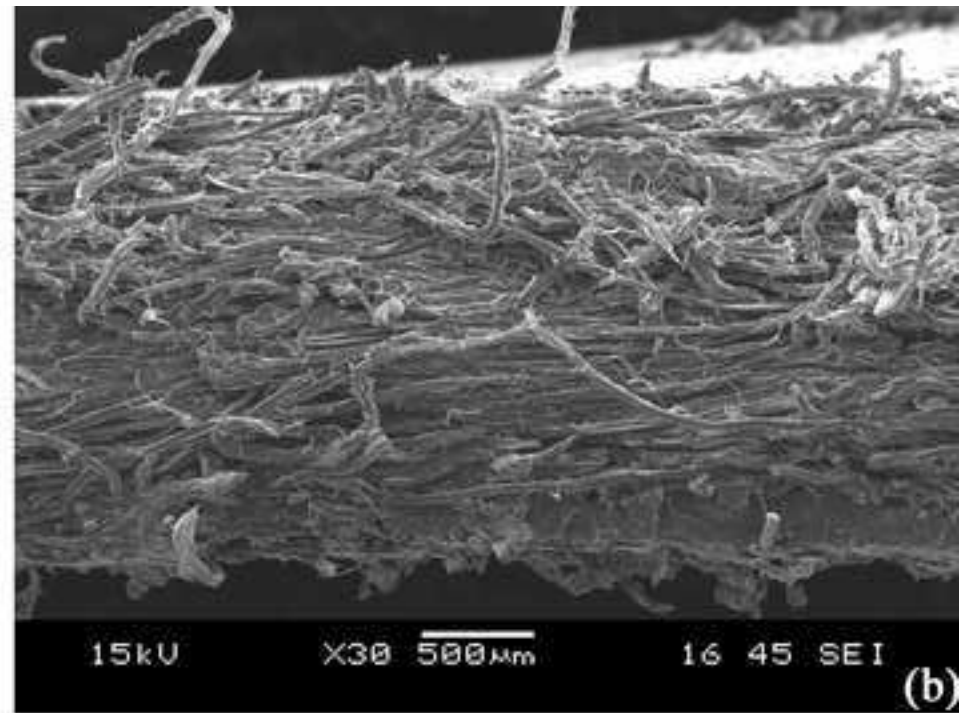
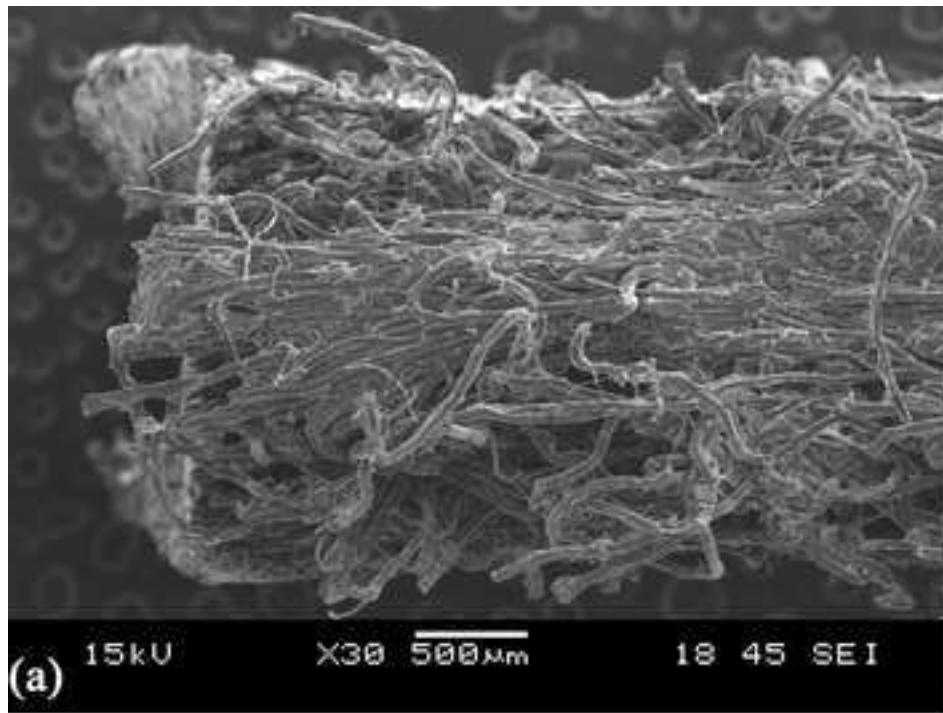


Figure_14
[Click here to download high resolution image](#)

